

Discovering protective T-cell responses by interrogating naturally processed antigenic determinants

Pavlo Gilchuk¹, Charles T. Spencer¹, Stephanie B. Conant¹, Timothy Hill¹, Jennifer J. Gray¹, Xinnan Niu¹, Mu Zheng¹, John J. Erickson¹, Kelli L. Boyd¹, K. Jill McAfee¹, Carla Oseroff⁴, Sine R. Hadrup⁵, Jack R. Bennink⁷, William Hildebrand⁸, Kathryn M. Edwards², James E. Crowe, Jr.^{1,2}, John V. Williams^{1,2}, Søren Buus⁶, Alessandro Sette⁴, Ton N.M. Schumacher⁹, Andrew J. Link^{1,3} and Sebastian Joyce¹

¹Departments of Pathology, Microbiology and Immunology, ²Pediatrics, and ³Biochemistry, Vanderbilt University School of Medicine, Nashville, TN 37232; ⁴Centre for Infectious Diseases, Allergy and Asthma Research, La Jolla Institute of Allergy and Immunology, La Jolla, CA 92037; ⁵Centre for Cancer Immunotherapy, Department of Hematology, Herlev Hospital, Herlev, Denmark; ⁶Laboratory of Experimental Immunology, University of Copenhagen, Copenhagen, Denmark; ⁷Cellular Biology and Viral Immunology Section, Laboratory of Viral Diseases, National Institutes of Allergy and Infectious Diseases, National Institutes of Health, Bethesda, MD 20892; ⁸Department of Microbiology and Immunology, University of Oklahoma Health Science Centre, Oklahoma City, OK 73190; ⁹Division of Immunology, The Netherlands Cancer Institute, Amsterdam, The Netherlands

Table of Contents

1. Methods.....	2–7
2. Supplementary Tables.....	6–23
a. Table S1	6–11
b. Table S2	12
c. Table S3	13–20
d. Table S4	21–22
e. Table S5	23
3. Supplementary Figures with Legends.....	24–49
a. Figure S1	24
b. Figure S2	26
c. Figure S3	28
d. Figure S4	30
e. Figure S5	32
f. Figure S6	34
g. Figure S7	36
h. Figure S8	38
i. Figure S9	40
j. Figure S10	42
k. Figure S11	44
l. Figure S12	46
m. Figure S13	48
4. Supplementary Literature Cited.....	50

Methods

Plasmids

Constructs encoding biotin ligase (BirA), human β 2m, HLA-A*02;01 and B*07;02 heavy chains for expression in *Escherichia coli*, and soluble HLA class I production in mammalian cells, were previously described (1-5). Constructs encoding hybrid HLA-A*0201 and -B*0702 heavy chains were designed by replacing their α 3 domain residues 206–299 (NCBI RefSeq NM_002116.6 and NM_005514.6) with mouse H2K^b α 3 domain residues 203–296 (NCBI RefSeq NM_001001892.2). VACV ORFs were PCR amplified from cloned genome fragments (Addgene) to express truncated subunits A34R₂₁₋₁₆₈, D1R₅₆₅₋₈₄₄, J6R₁₈₈₋₄₆₆, A3L₆₂₋₃₁₉, L4R₃₃₋₂₄₉, F4L₁₋₃₁₉, D5R₃₃₀₋₄₇₀ and E2L₂₆₋₃₀₁ as C-terminal histidine-tagged fusion proteins from the *pET24a* plasmid (Merck; see Fig. S6).

Peptides

Large scale peptide syntheses and RPC purification was performed by the manufacturer (Schafer-N, Copenhagen, Denmark). Sequences of synthetic peptides were confirmed by mass spectrometry. Peptides were reconstituted in 100% DMSO at a concentration of 4.4mM and used at 100pM–20 μ M for various assays. Measurement of peptide/MHC class I dissociation and determination of $t_{1/2}$ was performed using scintillation proximity assay as previously described (6).

Expansion of epitope-specific T cells in PBMC with antigenic peptides

Frozen aliquots of PBMC were thawed at 37°C and incubated with DNase I (15–30 seconds) before washing with RPMI 1640 medium (Mediatech) supplemented with 5% (vol/vol) heat-inactivated normal human sera (Pel-Freez,), 2mM L-glutamine, 100U/ml of penicillin and 100U/ml of streptomycin (Mediatech). PBMC were rested overnight in 14 ml snap-top round bottom tubes at 3x10⁶/ml at a 30° angle. PBMC were expanded with 1 of 5 pools of peptides (Table S4). Each peptide (22 nM) was added to the rested PBMC along with 5 U/ml rhIL-2 (Teceleukin, NCI-BRB). IL-2 was replenished every other day through the first 7 days of culture at 5 U/ml. After a 5-day rest, PBMCs were washed, counted, and stained with tetramers or restimulated with individual peptides from the stimulating pool in the ELISpot format.

For use as effectors in antigen presentation assay, anti-VACV memory TCD8 cells were expanded from mouse spleen with individual antigenic peptides using the same protocol described for the expansion of human T cells from PBMC.

Generation of peptide–HLA class I tetramers

Recombinant heavy and light chain production (1), class I refolding with cognate conditional peptide ligands (2), biotinylation and purification (3), UV-mediated exchange of conditional peptide with VACV-derived peptides and quantification of peptide exchange (7) were performed as described previously. Class I multimerization with PE-, APC-, QDot605-, and QD655-streptavidin conjugated fluorochromes (Invitrogen) were performed as described (7, 8).

Tetramer and antibody staining

Lymphocytes from various mouse tissues were incubated with PE- and APC-labeled hybrid p/class I tetramers (0.1-1 µg/ml) and anti-CD8α-PerCP-Cy5.5 (clone 53-6.7), -B220- FITC (clone RA36B2) and -CD4-FITC (clone H129.19) antibodies for 1hr at room temperature in PBS containing 2% FBS (HyClone) and 50 nM Dasatinib (LC Laboratories). Phenotypic analysis of TCD8 was performed by co-staining with p/class I-QDot605/QDot655 multimers and anti-CD8α-Pacific Blue, -B220-FITC, -CD44-APC (clone IM7), -CD62L-APC-Cy7 (clone MEL-14), -CD127-PE (clone SB/14; all from BD Bioscience) or anti-KLRG-1-APC (clone 2F1; eBioscience). In some experiments p/class I tetramer⁺ TCD8 were analyzed for expression of intracellular GzmB (clone GB11,PE-labeled; Invitrogen). Epitope-specific immune T cell repertoires were analyzed by co-staining magnetically purified TCD8 with p/class I tetramers and a panel of FITC-conjugated anti-TCR-Vβ antibodies (BD Bioscience). Flow cytometric data were acquired using a FACSCalibur or LSRII flow cytometer (BD Biosciences) and analyzed with FlowJo software (Tree Star).

Human PBMC were stained with PE- and APC-labeled p/class I tetramers as described previously (8) and with anti-CD8-Alexa Fluor 700 (clone 35B, Invitrogen), -CD4-FITC (clone RPA-T4), -CD14-FITC (clone M5E2), -CD19-FITC (clone HIB19) antibodies and propidium iodide to exclude dead cells (BD Bioscience).

TCD8 re-stimulation and intracellular cytokine staining (ICS)

Splenocytes from immune mice were re-stimulated in vitro for 6 hours with the indicated VACV peptides or irrelevant HLA-B*07:02-restricted HMPV-derived peptide APYAGLIMI at 1–10 µg/ml in the presence of 10µg/ml brefeldin A (Sigma-Aldrich), GolgiStop (BD Bioscience), and anti-CD107a-Alexa Flour 488 (clone eBioH4A3; eBioscience). Cells were then stained with antibodies for surface expression of CD8 (Pacific Blue), CD3 (PerCP Cy5.5; clone 145-2C11) and B220 (APC-Cy7), followed by staining for intracellular IFN-γ (clone XMG1.2, APC), TNF-α (clone MP6-XT22, PE) or IL-2 (clone JES6-5H4, PE; all from BD Bioscience) and analyzed using flow cytometry.

Antigen presentation assay

To prepare stimulators, 2×10^8 naïve splenocytes were treated overnight with 10 ng/ml LPS. Cell cultures were inoculated with MOI=10 VACV in 7 ml RPMI 1640 + 1% BSA for 1 hour at 37°C followed by dilution to 50 ml RPMI 1640 + 10% FBS. At the indicated time points, brefeldin A was added to 10 µg/ml and cells were placed on ice. To probe for antigen presentation, 10^6 stimulators were incubated for 4 hours with 500-1000 TCD8 expanded *ex vivo* as described above. TCD8 cells were stained for intracellular IFN-γ and TNF-α and analyzed using flow cytometry.

Enumeration of naïve epitope-specific TCD8 populations

Enumeration of epitope-specific precursor TCD8 from naïve B7^{tg} mice was adapted from a method described previously (9). In brief, cells from pooled spleens and lymph nodes (LN) were enriched to >85% TCD8 by negative selection (Miltenyi Biotech), stained with anti-CD8α, -CD3ε, -B220, -CD4, -CD44, -CD62L antibodies and various PE-conjugated p/class I tetramers (0.1–1 µg/ml) followed by incubation with anti-PE microbeads (Miltenyi Biotech) to further enrich for the p/class I tetramer-positive fraction by magnetic sorting, and analysed by flow cytometry. p/B7.2 tetramer⁺ cells were identified as shown in Figure S11. The absolute number of naïve precursors per mouse was determined as described (9) and their frequency was normalized using the following equation: naïve frequency = (number of naïve precursors/CD8α⁺ T cell number) × 10⁶.

Obtaining recombinant VACV proteins

VACV proteins were produced in *E. coli* BL21(DE3), purified from inclusion bodies by Ni-affinity chromatography (GE Healthcare) to >90%, dialyzed in PBS, adjusted to 2 mg/ml with PBS/0.05% SDS and stored at -20°C.

Mouse immunization and lethal VACV challenge

Bone marrow-derived DCs were generated using modification of previously described approach (10). Briefly, bone marrow was obtained from the femurs and tibiae of B7^{tg} mice, erythrocytes lysed, and resuspended at 10^6 cells/ml in DC Media consisting of RPMI-1640 supplemented with 5% (vol/vol) heat-inactivated FBS (HiClone) 2mM L-glutamine, 100U/ml of penicillin, 100U/ml of streptomycin (Mediatech), 20ng/ml rmGM-CSF and 10ng/ml rmIL-4 (Peprotech). After 3 days, 75% of the media was replaced with fresh DC Media. After 6 days, cells were counted and re-plated. On d7, 100ng/ml LPS (Sigma) and 10µM peptide were added to the culture and incubated overnight to mature and to load the DCs with epitope, respectively. On d8, DCs were collected, counted and resuspended in PBS. By this time >85% of cells were CD11c^{HI} as determined by flow cytometry.

For determination of epitope-specific protection, mice were primed s.q. with 1×10^6 peptide-loaded DCs and then boosted in two weeks later i.v. with 200 μ g peptide formulated with 50 μ g of poly-IC (HMW, Invitrogen) and 50 μ g of anti-CD40 mAb (clone HB14, Bio X cell) in 200 μ l of PBS. In some experiments mice were primed with peptide, then boosted with peptide-loaded DCs and peptide.

For lethal respiratory challenge, mice were inoculated i.n. with 50 μ L PBS containing $\sim 10^6$ pfu VACV-WR under ketamine/xylazine anesthesia, weighed daily, scored for morbidity (0, no signs of illness or slight fur ruffling; 1, fur ruffling and back arching; 2, extensive fur ruffling and hunched posture; 3, lethargic; 4, death occurred between watch or euthanized after the loss of >30% of initial body weight. Six and 15 days post-challenge, TCD8 response was analyzed. Lungs were collected at d6 p.i. for determination of viral titers.

For protein immunization, groups of B7^{tg} mice were injected i.p. twice with 20 μ g of individual protein subunits formulated with 1 μ g α -galactosylceramide (Funakoshi Co) in PBS/0.01% SDS buffer. TCD8 response was analyzed as described above.

Histology and immunohistochemistry

Harvested lungs were fixed in 10% formalin, embedded in paraffin, 5 μ m-thick sections cut, and stained with hematoxylin and eosin (H&E). Immunohistochemistry for T cell infiltration of lungs sections was performed on the Leica Bond Max IHC stainer. Slides were deparaffinized. Heat induced antigen retrieval was performed on the Bond Max using their Epitope Retrieval 2 solution for 20 min. Slides were incubated with anti-CD3 (Santa Cruz, Inc. Santa Cruz CA) for one hour at 1:600 dilution. The Bond Intense R detection system was used for visualization. Stained tissue sections were examined using an Olympus BX41 microscope with Plan Achromat objectives 20X/0.5, 60X/0.90; images were captured with a Spot Flex digital camera using Diagnostic Instruments Spot Advanced acquisition software. Adobe Photoshop was utilized for white balancing and resizing of images.

VACV burdens

Lungs from individual mice were homogenized and sonicated prior to plating serial 10-fold dilutions on confluent BSC-40 cells. VACV plaques were visualized as above.

Supplementary Table 1. Characterization of vaccinia viral determinants presented during active infection

A. A*02;01

VACCC ORF ^a	Sequence	Prior reports ^b	C _n ^c	DPI ^d	# Hits ^e	Function ^f	Temporal. Exp ^g	T _{1/2, h}	VARV ⁱ	MONPV	ECTV
A2L ₁₁₄₋₁₂₂	QVKDEKLNL		2.376	1,2,3	7	T	L	14.59			
A3L ₁₂₉₋₁₃₇	LNIMNKLNI		2.820			S	L	14.26			
A6L ₆₋₁₄	VLYDEFVTI	Am	2.018			S	L	14.11			
A6L ₁₇₁₋₁₇₉	ILSDENYLL	AMh	1.925	1,3	6	S	L	24.41			
A7L ₁₉₂₋₂₀₀	KIIQRVQDL		2.021	1,2	3	T	L	1.19			
A7L ₂₂₄₋₂₃₂	ILNDEQLNL		2.951	1,2,3	17	T	L	6.37			
A7L ₂₄₉₋₂₅₇	TVMINNVKL		2.206	1,2,3	4	T	L	0.78			
A7L ₄₆₂₋₄₇₀	QIDVEKKIV		2.106	1,2	4	T	L	13.31			V9P ^j
A7L ₅₇₁₋₅₇₉	LIQEIVHEV	M	2.535	1,3	3	T	E	19.13			
A8R ₁₃₄₋₁₄₂	QVSIIQEKL		2.185	1,2,3	6	T	IE	0.11			
A10L ₇₆₋₈₅	YLIDTTSREL		2.020	2,3	3	S	L	9.77			E8S
A10L ₇₄₀₋₇₄₉	MLVSQALNS V		1.523			S	L	14.19	N8D	N8D	N8D
A11R ₂₆₀₋₂₆₉	KLGFEETKGL		2.103	2,3	7	O	L	5.6	E5D		
A11R ₂₉₂₋₃₀₀	KLGIGNSPV		1.626	1	7	O	L	3.13			
A13L ₆₁₋₇₀	SLYNLVKSSV		1.895	1,3	5	S	L	6.36		V10A	V10A
A24R ₁₁₁₇₋₁₁₂₆	KIDTTHVSKV		2.190	1,2	4	T	E	4.06			
A27L ₄₆₋₅₄	TLKQRLTNL	Am	1.607		1	S	L	0.95			
A29L ₁₅₇₋₁₆₅	KLTFLDVEV		1.630	2,3	4	T	E	5.93			
A31R ₆₈₋₇₆	TINDLKMM		1.822	1,2,3	8	U	E	0.96			
A36R ₁₋₉	MMLVPLITV	Amh	1.070			S	E	14.14	M2I		
A37R ₁₅₃₋₁₆₁	YLPLSVFII		1.606			U	IE	2.82	NSH		
A39R ₁₃₋₂₁	FVDVIIKV		1.892	1	1	E/V	L	3.57	NSH	NSH	
A39R ₃₉₄₋₄₀₂	MPQMKKILK		2.163			E/V	L	1.05	NSH	NSH	M1I Q3R
A44L ₃₀₆₋₃₁₄	KISNTTFEV		2.495	1,2,3	6	E/V	IE	18.51	V9A		T6A
A48R ₂₁₀₋₂₁₈	IVIEAIHTV	Mh	3.251	1,2,3	10	R	IE	6.66			I6M
A50R ₄₅₈₋₄₆₆	TLRVLQDQL		2.342	2	1	R	E	0.19			
A51R ₂₇₋₃₅	MIKPCCERV		2.012	1	1	U	E	3.46			
A52R ₉₆₋₁₀₄	TIEELKQKL		2.258	1,2,3	6	E/V	IE	14.09		NSH	
B8R ₁₀₁₋₁₀₉	KIGPPTVTL		2.241	1,2	8	E/V	E	1.53			
B13R ₃₂₇₋₃₃₅	HVDGKILFV	Am	2.182	3	2	E/V	IE	4.22			
B19R ₂₅₄₋₂₆₂	LILDPKINV		2.143	1,2,3	5	E/V	E	1.06	P5S		
B19R ₂₉₄₋₃₀₂	WLIGFDVD	Ah	1.859	3	5	E/V	E	23.56		NSH	
B20R ₂₈₈₋₂₉₇	YLLDRGADIV		2.355	1,2,3	18	U	E	ND			
B23R and C17L ₂₆₄₋₂₇₂	DIEIVKLLL		1.659	1	2	U	N/A	ND	E3D L9M	E3D L9M	NSH

VACCC ORF ^a	Sequence	Prior reports ^b	Cn ^c	DPI ^d	# Hits ^e	Function ^f	Temporal Exp ^g	t _{1/2} , h ^h	VARV ⁱ	MONPV	ECTV
C1L ₂₇₋₃₅	ILMRHLKNL		2.064	1	1	U	E	16.08	H5Y		NSH
C2L ₁₂₄₋₁₃₂	EIINNITAV		2.060	2,3	2	E/V	E	0.68	NSH		
C4L ₂₀₂₋₂₀₉	LLVNEFYI		1.833			U	E/L	6.79	I8T		NSH
C5L ₉₉₋₁₀₇	YINNNIEEI		2.250			U	E/L	4.14			NSH
C7L ₇₄₋₈₂	KVDDTFYYV	AM mh	2.267	1,2,3	7	U	E	12.21		D4Y	
C9L ₆₀₂₋₆₁₀	KIDDMIEEV		2.226	1,2,3	8	U	E/L	9.54	D4N E7N	M4N E7D	NSH
C12L ₁₆₋₂₄	VLISPVSIL		1.923	1,2,3	4	E/V	E	0.46			
C12L ₂₉₂₋₃₀₀	FLHTTFIDV		1.715	1,2	2	E/V	E	ND	T4K	T5A	
D1R ₃₃₋₄₁	EINNELELV		2.427	1,2	4	T	E	0.83			
D1R ₂₅₁₋₂₅₉	RVYEALYYV	AM mh	1.822	1,2	4	R	E	14.44			
D1R ₇₆₄₋₇₇₂	YIIKKNDIV		1.582	1	1	T	E	0.78			
D2L ₁₈₋₂₇	ILFPDDVQEL		2.606	1,2,3	6	S	L	5.09	E9K	V7L	
D2L ₇₇₋₈₅	LLFLKDVEP		2.503		0	S	L	29.02	K5E	K5E	K5E
D5R ₅₆₈₋₅₇₇	KIRSDNIKKL		2.385	2	1	R	E	6.85			
D8L ₁₅₅₋₁₆₄	YLDNLLPSTL		2.189	2	2	S	L	0.98	T9K		
D10R ₁₆₈₋₁₇₆	TIINKFFEV		2.419	1	1	O	IE	ND			
D12L ₁₇₄₋₁₈₂	SLFKNVRL	Ah	2.005	1,2,3	3	T	E	1.29			
D12L ₆₂₋₇₀	KLFTHDIML	AM mh	1.602			T	E	22.82			
D13L ₁₇₂₋₁₈₀	KLSDSKITV		2.572	1,2,3	13	O	L	27.07			
D13L ₃₂₇₋₃₃₅	DVYVKIDNV		1.979	1,2,3	4	O	L	ND			
D13L ₆₂₋₇₀	YITALNHVL		2.567	1	4	O	L	16.66			
D13L ₇₀₋₇₈	VLSLELP	M	2.249	1,3	4	O	L	22.73			
E2L ₂₄₉₋₂₅₇	KIDYYIPYV	AM mh	2.091	1,3	3	U	E	22.12			V9A
E2L ₇₀₃₋₇₁₁	FIFLKKNEL		2.552	2,3	4	U	E	0.15			
E3L ₄₂₋₅₀	EVNKALYDL		1.883	1,2,3	45	E/V	IE	0.89			
E5R ₁₁₇₋₁₂₅	KLFSDISAI	Mh	2.338			R	IE	17.75			
E5R ₂₅₂₋₂₆₀	LVEKVLKIL		2.120	1,2	11	R	IE	11.08			
E6R ₄₆₂₋₄₇₀	YLDGQLARL		2.291	3	1	U	L	14.38			
E9L ₂₇₁₋₂₇₉	YITNRLELL		2.256	1,3	4	R	E	2.71			
E9L ₉₇₈₋₉₈₇	EIVNLLDNKV		1.853	3	5	R	E	ND			
F1L ₁₂₅₋₁₃₃	TVYDINNEV		2.141	2,3	2	U	E	2.84			E8K
F10L ₂₅₄₋₂₆₃	PLALYSADKV		1.746	1	2	S	E	ND		A3V	
F10L ₃₀₇₋₃₁₅	DLKPDNILL		2.135	1,3	5	S	E	ND			
F11L ₃₄₀₋₃₄₈	SLSNLDFRL	M	2.728	1,2,3	65	U	E	23.58	R8Y		
F12L ₂₅₁₋₂₆₀	FVNFSVKNL		2.051	1,3	7	S	E	0.43	N9D	N9D	N9D
F12L ₂₈₆₋₂₉₅	NLFDIPLLT	AM mh	1.639	3	1	S	E	22.59			
F12L ₄₀₄₋₄₁₂	FLTSVINRV	AM mh	1.692			S	E	19.28			
F13L ₁₄₀₋₁₄₉	SIHTIKTLGV		1.663		2	S	L	0.35			

VACCC ORF ^a	Sequence	Prior reports ^b	Cn ^c	DPI ^d	# Hits ^e	Function ^f	Temporal Exp ^g	t _{1/2} , h ^h	VARV ⁱ	MONPV	ECTV
F14L ₃₉₋₄₇	ELLNLTEL		2.347	1,2,3	7	U	E	0.88			
G3L ₉₉₋₁₀₈	DIRTLLPILL		2.248	1,2,3	4	S	L	7.12			
G4L ₅₇₋₆₆	TLIGNFAAHL		2.226	3	4	S	L	9.86			
G5R ₁₈₋₂₆	ILDDNLYKV	Amh	3.437	1,2,3	12	U	IE	26.21			K8N
G5R ₁₂₄₋₁₃₂	EMQLKIDKL		2.276	1,2,3	7	U	IE	0.81	M2I		
G5.5R ₂₇₋₃₅	SLKDVLVSV	Mh	2.052	1,2	4	T	E	13.79			
G7L ₁₆₁₋₁₆₉	EMKYALINL		2.165	1,2,3	21	S	L	AMB			
G9R ₁₁₃₋₁₂₁	VLESCWPDV		1.843	1,2,3	8	S	L	0.93			V1E V9A
G8R ₂₅₁₋₂₅₉	KINIFMAFL		1.898	1,3	3	N/A	N/A	1.91			
H3L ₁₈₄₋₁₉₂	SLSAYIIRV	Amh	2.669	1,2,3	28	S	L	25.52			
H4L ₆₇₆₋₆₈₄	KIEIERKKL		2.309	1,2,3	9	T	L	13.46			
H5R ₁₅₉₋₁₆₈	VLEDVQAAGI	Am	1.507			T	E	0.35			
H6R ₃₋₁₁	ALFYKDGKL		1.621	2,3	3	T	E/L	0.35			A1P
I1L ₁₂₂₋₁₃₀	YIDISDVKV		2.631	3	2	S	L	0.82			
I1L ₁₅₅₋₁₆₃	KIEDLINQL		2.444	1,2,3	4	S	L	0.35			
I1L ₂₁₁₋₂₁₉	RLYDYFTRV	Amh	2.621	1,2,3	13	S	L	20.03			
I3L ₂₁₂₋₂₂₀	KLIIDREVV		1.794	3	3	R	IE	AMB			
I7L ₃₆₄₋₃₇₂	KMTLFKSIL		2.416	1,2	3	S	L	0.42			
I8R ₄₂₇₋₄₃₅	KVLDIDEIL		2.520	1,2,3	7	T	E	0.55	D4E E7K		
I8R ₄₃₀₋₄₃₈	DIDEILEKV		2.510	1	3	T	E	13.38	D1E E4K		
J6R ₃₇₅₋₃₈₄	SIIFGRQPSL		2.009	2	1	T	E	0.99			
J6R ₅₉₃₋₆₀₁	AINVEKIEL		2.044	1,2	3	T	E	0.20			
J6R ₆₅₃₋₆₆₁	LIDNPNDNNL		2.230			T	E	0.76			N4D
J6R ₇₁₇₋₇₂₆	YILNSLTKGL		2.347	1,2,3	10	T	E	1.66			
J6R ₁₀₇₄₋₁₀₈₂	FVEPEELNL		2.543	1,2	3	T	E	0.94			
K1L ₁₉₁₋₂₀₀	SLLFIPDIKL	M	2.487	3	1	U	IE	14.13	S1F		
K3L ₅₇₋₆₅	KLVGKTVKV	M	2.185	1,3	3	E/V	IE	20.50		NSH	T6K
L3L ₁₄₂₋₁₅₀	KVVKLTPQV		1.956	1,2,3	4	T	L	3.85	K4R	K4R	K4R
L3L ₁₈₂₋₁₉₁	LVSIPRTNIV		1.869	1,3	3	T	L	10.83			
O1L ₂₄₇₋₂₅₅	GLNDYLHSV	AM mh	2.493	3	1	U	IE	48.96			
O1L ₅₅₀₋₅₅₉	PITDSLSFKL		2.369	2,3	2	U	IE	ND	D4E		
O1L ₅₆₆₋₅₇₄	VLNDQYAKV		2.982	1,2	4	U	IE	18.05			
AorfA ₁₀₂₋₁₁₀	YLFLICHNL		2.496	1,2,3	12	N/A	N/A	8.23	NSH	NSH	NSH
AorfU ₅₉₋₆₇	RIIYIIRFL		2.543	3	3	N/A	N/A	0.83	NSH	NSH	NSH
IorfA ₆₆₋₇₄	YLSAKITTL		1.652	1	1	N/A	N/A	12.31	NSH	NSH	NSH
VAC WR148 ₄₃₃₋₄₄₁	KLTELNAEL		2.809	1,3	7	S	L	38.27		A7E	NSH
VAC WR148 ₄₃₆₋₄₄₅	ELNAELSDKL		2.133	1,2,3	8	S	L	ND		A4E	NSH

B. B*07;02

ORF ^a	Sequence	Prior reports ^b	Cn ^c	DPI ^d	# Hits ^e	Function ^f	Temporal Exp ^g	t _{1/2, h} ^h	VARV ⁱ	MONPV	ECTV
A3L ₁₉₂₋₂₀₀	SPSNHHILL		1.917	1,3	4	S	L	5.45			
A3L ₄₅₃₋₄₆₂	SPVIVNGAMM		1.377	1,2	2	S	L	0.62			
A4L ₈₃₋₉₁	VPTATPAPI		1.686	1,2,3	27	S	E/L	0.83	NSH ^j	A4P	NSH
A4L ₁₂₆₋₁₃₅	APASSLLPAL		2.110	1,3	6	S	E/L	2.71	NSH	S5T	NSH
A10L ₁₁₁₋₁₂₀	NPIINTHSFY		1.732	2,3	3	S	L	ND			S8N
A10L ₁₂₂₋₁₃₀	LPPFTQHLL		1.843	2,3	2	S	L	0.24			
A11R ₂₂₋₃₀	YPSNKNYEI		2.005	3	1	O	L	1.19			
A16L ₃₃₀₋₃₃₉	EPVVKDKIKL		2.317	1,3	2	S	L	ND		K5N	
A20R ₁₆₂₋₁₇₀	IPKYLEIEI		1.960	1,2	14	R	E	0.43	K3N	K3N	
A24R ₁₀₀₂₋₁₀₁₀	KPYASKVFF		1.924	1,2,3	5	T	E	5.43		A4E	
A34R ₈₂₋₉₀	LPRPDTRHL	Am	2.002	1,2,3	14	S	L	7.13		R3G	
A40R ₃₋₁₁	KPKTDYAGY		1.941	2	1	E/V	E	ND	D5N	NSH	NSH
A40R ₈₈₋₉₆	NPNSDLIKI		1.137	1	2	E/V	E	ND	NSH	NSH	
A47L ₂₂₇₋₂₃₆	KPVSDLYTSM		1.850	1	3	U	IE	3.19		NSH	
B8R ₇₀₋₇₈	FPKNDFVSF		2.237	1,3	3	E/V	E	5.20			K3N
B8R ₁₅₈₋₁₆₇	EPVTYDIDDY		2.047	1,3	2	E/V	E	ND	D6N		T4I
B12R ₂₅₁₋₂₅₉	EPELEVRYI		2.082	2	1	U	IE	ND	NSH		
B16R ₂₂₆₋₂₃₄	LPDGIVTSI		1.932	1,2,3	9	E/V	L	0.59	NSH	D3E I5V	
B17L ₁₈₂₋₁₉₁	APLPGNVLVY		1.802	1,3	6	U	E	ND	L3Y	NSH	
B18R ₃₀₅₋₃₁₃	RPADSITYL		1.690	1,2,3	6	U	E	3.16	A3L	NSH	R1H A3S
C19L and B25R ₇₈₋₈₆	NPSVLKILL		1.702	2,3	4	U	E	0.22	N1K		N1K
C10L ₄₁₋₄₉	LPMEDNSDI		1.692	1,3	2	U	E	N/A			
C10L ₄₁₋₅₀	LPMEDNSDII		1.829	1	2	U	E	1.38			
C20L and B26R ₇₋₁₆	EPIRGYVIIIL		2.020	2,3	3	P	E	ND	NSH	NSH	NSH
D11L ₁₀₂₋₁₁₁	APEITKDCIF		1.740	2,3	4	T	L	0.94			
D1R ₃₈₄₋₃₉₃	GPKSNIDFKI		2.185	1	1	T	E	ND			
D1R ₈₀₈₋₈₁₇	RPSTRNFFEL	Am	1.549	1	1	T	E	2.93			
D5R ₃₆₁₋₃₆₉	EPLITKLIL		1.578	1,3	3	R	E	ND			
D5R ₃₇₅₋₃₈₃	LPKEYSSEL		1.885	1	2	R	E	7.44			
D8L ₁₆₀₋₁₆₉	LPSKLDYFTY		1.843	3	1	S	L	ND	T9K	K4T	K4T
D9R ₂₆₋₃₅	IPRSKDTHVF		2.080	2,3	5	O	IE	5.37			
D9R ₁₀₀₋₁₀₉	DPHFEELILL		2.066	1	1	O	IE	ND			
D11L ₅₀₆₋₅₁₄	MPTVDEDLF		1.652	1,3	2	T	L	0.84			
E1L ₁₀₋₁₈	LPNITLKII		1.539	1,2	3	T	E	0.86			
E2L ₂₁₆₋₂₂₄	RPRDAIRFL		2.049	3	1	U	E	4.81			

VACCC ORF ^a	Sequence	Prior reports ^b	Cn ^c	DPI ^d	# Hits ^e	Function ^f	Temporal Exp ^g	t _{1/2} , h ^h	VARV ⁱ	MONPV	ECTV
E5R ₁₃₁₋₁₄₀	NPSKMYVALL		1.567	1,3	2	R	IE	0.39	V6A		
E6R ₂₈₄₋₂₉₃	EPEKDIRELL		1.836	3	1	U	L	2.71			
E9L ₁₇₅₋₁₈₃	FPSVFINPI		1.594	1,3	2	R	E	2.40			
E9L ₅₂₆₋₅₃₄	FPYEGGKV		1.845	3	3	R	E	6.17			
F2L ₂₆₋₃₅	SPGAAGYDLY		1.537	1,2,3	7	R	E	ND	G3Y		NSH
F2L ₄₂₋₅₀	IPPGERQLI		1.657	1,2	2	R	E	ND			
G2R ₁₄₀₋₁₄₉	VPITGSKLIL		2.260	2	1	T	E	1.19	T4A	T4A	NSH
G5R ₃₄₁₋₃₄₉	LPCQLMYAL		2.034	2	1	U	IE	3.52			
G7L ₁₇₅₋₁₈₃	LPMIIGEPI		2.086	2,3	3	S	L	5.02			
G9R ₁₄₋₂₃	PPPGVPTDEM		1.214	1,3	2	S	L	ND			
G9R ₆₉₋₇₇	GPGGLSALL		1.583	2,3	3	S	L	0.37			G4N
H1L ₆₅₋₇₃	LPNSNIIII		2.141	1,2,3	4	T	E/L	1.01			
H3L ₆₋₁₄	TPVIVVPVI		2.137	2	1	S	L	ND			V3I
H5R ₈₉₋₉₇	SPSPGVGDI		1.637	1,3	3	T	E	0.65	P2S	P2S	NSH
I1L ₁₈₄₋₁₉₂	IPDELIDVL		1.771	3	2	S	L	AMB			
I4L ₄₉₈₋₅₀₇	RPIGIGVQGL		2.975	2	3	R	E	ND			
I6L ₂₃₇₋₂₄₅	FPTNTLTSI		2.013	2	1	U	E/L	1.52			
I6L ₂₇₂₋₂₈₀	IPKKIVSSL		1.752	2	1	U	E/L	5.35			
I6L ₂₈₂₋₂₉₁	LPSNVEIKAI		1.769	1	1	U	E/L	0.54			
I7L ₃₄₂₋₃₅₀	TPPKSFKSL		1.900	2	2	S	L	0.85			
I8R ₂₂₁₋₂₃₀	RPVILSLPRI		1.057	2,3	2	T	E	2.35			
J3R ₈₋₁₆	KPFMYFEEI		1.800	1	1	T	E/L	1.24			
J3R ₂₅₃₋₂₆₁	YPNQEYDYF		1.656	1,3	2	T	E/L	ND			
J5L ₅₃₋₆₁	LPASLKKNI		2.220	2,3	2	S	L	ND			
J6R ₁₀₈₉₋₁₀₉₈	LPGAANKGKI		1.230	1,2	4	T	E	0.97			
J6R ₁₁₀₃₋₁₁₁₁	IPISDYTGY		2.019	1,3	10	T	E	ND			
K1L ₁₅₁₋₁₅₉	IPSTFDLAI		2.020	1,2,3	4	U	IE	0.71	NSH	T4F	
K6L ₁₇₋₂₅	KPITYPKAL		2.603	1,3	14	O	IE	4.99	NSH		
L4R ₃₇₋₄₅	FPRSMSLSIF		1.962	1	1	T	L	6.08			
N2L ₁₀₄₋₁₁₃	RPNQHHTIDL		2.007	3	1	O	IE	4.73			Q4K

^aOpen reading frames (ORF) and location of epitopes are defined based on Copenhagen reference strain (VACCC, ID 10249)

^bprior reports according to immune epitope data base (IEDB; www.iedb.org); A, algorithm based; M, discovered by MHC class I ligand elution; m, positive in mouse TCD8 assay; h, positive in human TCD8 assay; blank, this study

^ccorrelation coefficient represents the number of peak identities determined between the theoretically and experimentally derived spectra for a given parent ion normalized to the charge state of the peptide

^ddays p.i. of HeLa cultures with VACV at which the peptide was identified

^etotal number of times a given peptide sequence was identified by mass spectrometry

^fprotein function according to (11); S, structural (virion membrane and core); T, transcription; E/V, evasion/virulence; O, other; U, unknown; P, pseudogenes

^gtemporality of expression (shortened) according to (12): IE, immediate early; E; early; E/L, early/late; L, late; N/A, unidentified; ^hHalf-time of p/MHC stability. ND, no signal obtained; AMB, ambiguous, data from independent experiments were inconsistent. ND, not determined

ⁱpeptide homologies were identified using Netblast (blastcl3 at www.ncbi.nlm.nih.gov) using the following taxonomy id: VARV, variola virus, 10255; ECTV, ectromelia virus, 12643; MONPV, monkeypox virus, 10244)

^jAmino acid changes for homologous poxviral epitopes; NSH, no significant homology; blank, conserved sequences with 100 % homology.

Supplementary Table 2: Volunteer demographics, HLA haplotype and vaccination history

ID	Gender	Ethnicity	Age at vaccination	HLA-A*		HLA-B*		Time since vaccination
V101	M	Caucasian	22	0101	0301	0702	0801	4.5 months after primary
V111	M	Caucasian	51	0101	0201	0702	0702	4 months after boost
V115	M	Caucasian	34	0201	0201	4001	4101	3 months after boost
V150	F	Caucasian	61	0301	2301	0702	3701	10 months after boost
V154	F	Caucasian	28	0301	3201	0702	1501	3 months after primary
V155	F	Caucasian	30	0201	3201	0702		3 months after primary
V158	F	Caucasian	28	0301	3002	0702	4402	13 days after primary
V163	F	Caucasian	44	0201	0301	0702	1501	6 days after boost
V168	M	Caucasian	32	0205	6801	3902	5301	15 days after primary
V001	F	Caucasian	24	0201		1501	5101	4 years after primary
V003	F	Caucasian	27	0201	2901	0702	0705	4 years after primary
V008	M	Caucasian	60	0201	0301	1402	1404	4 years after primary
V023	F	Caucasian	25	0201	2402	1302	4001	4 years after primary
V034	F	Caucasian	30	0101	0201	0801	1302	3.5 month after boost

Supplementary Table 3. Peptide pools used for screening of TCD8 from VACV immune humans and HLA class I transgenic mice

A. A*02;01			
	ORF ^a	Peptide	Source ^b
Pool 1	J6R ₅₉₃₋₆₀₁	AINVEKIEL	MS
	A23R ₂₇₃₋₂₈₁	ALDEKLFLI	MS+
	H6R ₃₋₁₁	ALFYKDGLK	MS
	H3L ₁₄₂₋₁₅₁	AMHDKKIDIL	Predicted
	A27L ₉₂₋₁₀₀	AMISLAKKI	Predicted
	A55R ₃₉₁₋₃₉₉	AMLNGLIYV	Public
	B15R ₂₉₋₃₇	CLTEYILWV	Public
	G3L ₉₉₋₁₀₈	DIRTLLPILL	MS
	N/A	DVRTLLPILL	dMS
	F10L ₃₀₇₋₃₁₅	DLKP DNILL	MS
	N/A	DLKPENILL	dMS
	N/A	DIKP DNILL	dMS
	N/A	DLKPQ NILL	dMS
	E9L ₉₇₈₋₉₈₇	EIVNLLDNKV	MS
	VACWR148 ₄₃₆₋₄₄₅	ELNAELSDKL	MS
	G5R ₁₂₄₋₁₃₂	EMQLKIDKL	MS
	N/A	EIQLKIDKL	dMS
	A4L ₂₄₇₋₂₅₅	ETNDLVTVNV	Public
	E2L ₇₀₃₋₇₁₁	FIFLKKNEL	MS
	F12L ₂₅₁₋₂₆₀	FVN FNSVKNL	MS
	N/A	FVN FNSVKDL	dMS
	A46R ₁₄₂₋₁₅₀	GLFDFVN FV	MS+
	O1L ₂₄₇₋₂₅₅	GLNDYLHSV	MS+
	B13R ₃₂₇₋₃₃₅	HVDGKILFV	MS+
	G5R ₁₈₋₂₆	ILDDNLYKV	MS+
	D2L ₁₈₋₂₇	ILFPDDVQEL	MS
	A10L ₅₁₋₅₉	LLNNSLGSV	Predicted
	K1L ₁₅₉₋₁₆₇	ILLSCIHTT	Predicted
	A7L ₂₂₄₋₂₃₂	ILNDEQLNL	MS
	A6L ₁₇₁₋₁₇₉	ILSDENYLL	MS+
	A48R ₂₁₀₋₂₁₈	IVIEAIHTV	MS+
	A24R ₁₁₁₇₋₁₁₂₆	KIDTTHVSKV	MS
Pool 2	N/A	KVDTTHVSKV	dMS
	E2L ₂₄₉₋₂₅₇	KIDYYIPYV	MS+
	H4L ₆₇₆₋₆₈₄	KIEIERKKL	MS
	A44L ₃₀₆₋₃₁₄	KISNTTFEV	MS
	B8R ₁₉₋₂₇	ITSYKFESV	Predicted

ORF^a	Peptide	Source^b
E5R ₁₁₇₋₁₂₅	KLFSDISAI	MS+
D12L ₆₂₋₇₀	KLFTHDIMAL	MS+
A11R ₂₆₀₋₂₆₉	KLGFEIKGL	MS
N/A	KLGFDEIKGL	dMS
A11R ₂₉₂₋₃₀₀	KLGIGNSPV	MS
I3L ₂₁₂₋₂₂₀	KLIIDREVV	MS
B19R ₂₀₇₋₂₁₅	KLIHNPEL	Public
A29L ₁₅₇₋₁₆₅	KLTFLDVEV	MS
I7L ₃₆₄₋₃₇₂	KMTLFKSIL	MS
C7L ₇₄₋₈₂	KVDDTFYYV	MS+
A47L ₁₆₉₋₁₇₇	LLYAHINAL	Public
B6R ₁₀₈₋₁₁₆	LMYDIINSV	Public
A3L ₁₂₉₋₁₃₇	LNIMNKLDI	MS
L3L ₁₈₂₋₁₉₁	LVSIPRTNIV	MS
A10L ₇₄₀₋₇₄₉	MLVSQALNSV	MS
A36R ₁₋₉	MMLVPLITV	MS+
A10L ₁₋₁₀	MMPIKSIVTL	Predicted
A10L ₇₇₃₋₇₈₁	NLATSIYTI	Predicted
A27L ₅₃₋₆₁	NLEKKITNV	Public
F12L ₂₈₆₋₂₉₅	NLFIDIPLLT	MS+
A26L ₆₋₁₄	NLWNGIVPT	Public
E3L ₃₅₋₄₃	QLNMEKREV	Predicted
A4L ₂₇₁₋₂₈₀	QLVKGFERFQ	Public
A2L ₁₁₄₋₁₂₂	QVKDEKLNL	MS
I1L ₂₁₁₋₂₁₉	RLYDYFTRV	MS+
A13L ₆₁₋₇₀	SLYNLVKSSV	MS
A27L ₄₋₁₂	TLFPGDDDL	Public

Pool 3	A27L ₄₆₋₅₄	TLKQRLTNL	MS+
	C7L ₈₂₋₉₀	VIYEAVIHL	Predicted
	H5R ₁₅₉₋₁₆₈	VLEDVQAAGI	MS+
	A27L ₇₈₋₈₆	VLFRLLENHA	Public
	D6R ₄₉₈₋₅₀₆	VLPFDIKKL	Public
	A6L ₆₋₁₄	VLYDEFVTI	MS+
	A55R ₇₈₋₈₆	YIYGIPSL	Public
	D8L ₁₅₅₋₁₆₄	YLDNLLPSTL	MS
	A10L ₇₆₋₈₅	YLIDTTSREL	MS
	B20R ₂₈₈₋₂₉₇	YLLDRGADIV	MS
	G7L ₂₅₀₋₂₅₈	YLPEVISTI	Public
	N/A	GLFGFVNPF	dMS
	J6R ₆₅₃₋₆₆₁	LIDNPDNNL	MS
	D2L ₇₇₋₈₅	LLFLKDVEP	MS
	C4L ₂₀₂₋₂₀₉	LLVNEFYI	MS

ORF^a	Peptide	Source^b
A39R ₃₉₄₋₄₀₂	MPQMKKILK	MS
G5.5R ₂₇₋₃₅	SLKDVLVSV	MS+
I4L ₇₂₀₋₇₂₈	SMHFYGWSL	Public
C16L ₁₇₁₋₁₇₉	TLLDHIRTA	Public
A27L ₈₈₋₉₆	TLRAAMISL	Public
B19R ₂₉₄₋₃₀₂	WLIGFDVDV	MS+
I8R ₄₃₀₋₄₃₈	DIDEILEKV	MS
J6R ₁₀₇₄₋₁₀₈₂	FVEPEELNL	MS
D13L ₁₇₂₋₁₈₀	KLSDSKITV	MS
I8R ₄₂₇₋₄₃₅	KVLDIDEIL	MS
F11L ₃₄₀₋₃₄₈	SLSNLDFRL	MS
O1L ₅₆₆₋₅₇₄	VLNDQYAKV	MS
I1L ₁₂₂₋₁₃₀	YIDISDVKV	MS
D13L ₆₂₋₇₀	YITALNHLV	MS
E5R ₂₅₂₋₂₆₀	LVEKVLKIL	MS
D12L ₂₅₁₋₂₅₉	RVYEALYYV	MS+
H3L ₁₈₄₋₁₉₂	SLSAYIIRV	MS+

Pool 4	G9R ₁₁₃₋₁₂₁	VLESCWPDV	MS
	C5L ₉₉₋₁₀₇	YINNNIEEI	MS
	E9L ₂₇₁₋₂₇₉	YITNRLELL	MS
	F12L ₄₀₄₋₄₁₂	FLTSVINRV	MS+
	G8R ₂₅₁₋₂₅₉	KINIFMAFL	MS
	N/A	LLFLEDVEP	dMS
	VACCA ₁₇₇₋₁₈₆	*YLYTEYFLFI	Predicted
	A7L ₅₇₁₋₅₇₉	LIQEIVHEV	MS
	N2L ₉₃₋₁₀₁	YVNAILYQI	Public
	D13L ₃₂₇₋₃₃₅	DVYVKIDNV	MS
	D1R ₃₃₋₄₁	EINNELELV	MS
	F14L ₃₉₋₄₇	ELLNILTEL	MS
	G7L ₁₆₁₋₁₆₉	EMKYALINL	MS
	E3L ₄₂₋₅₀	EVNKALYDL	MS
	A10L ₄₄₋₅₂	FHVPDFILL	Predicted
	A39R ₁₃₋₂₁	FVDVIIKV	MS
	C9L ₆₀₂₋₆₁₀	KIDDMIEEV	MS
	I1L ₁₅₅₋₁₆₃	KIEDLINQL	MS
	B8R ₁₀₁₋₁₀₉	KIGPPTVTL	MS
	N/A	KISYYIPYV	dMS
	VACWR148 ₄₃₃₋₄₄₁	*KLTELNAEL	MS
	L3L ₁₄₂₋₁₅₀	KVVKLTPQV	MS
	B19R ₂₅₄₋₂₆₂	LILDPKINV	MS
	A7L ₄₆₂₋₄₇₀	QIDVEKKIV	MS
	A52R ₉₆₋₁₀₄	TIEELKQKL	MS

ORF^a	Peptide	Source^b
C12L ₁₆₋₂₄	VLISPVSIL	MS
J6R ₇₁₇₋₇₂₆	YILNSLTGKL	MS
A37R ₁₅₃₋₁₆₁	YLPLSVFII	MS
I orf A ₆₆₋₇₄	YLSAKITTL	MS
B23R and C17L ₂₆₄₋₂₇₂	DIEIVKLLL	MS
C12L ₂₉₂₋₃₀₀	FLHTTFIDV	MS

Pool 5	C2L ₁₂₄₋₁₃₂	EIINNITAV	MS
	C1L ₂₇₋₃₅	ILMRHLKNL	MS
	A7L ₁₉₂₋₂₀₀	KIIQRVQDL	MS
	VACWR148 ₄₃₃₋₄₄₁	KLTELNAEL	MS
	A7L ₅₇₁₋₅₇₉	LIQEIVHEV	MS
	A51R ₂₇₋₃₅	MIKPCCERV	MS
	F10L ₂₅₄₋₂₆₃	PLALYSADKV	MS
	A orf U ₅₉₋₆₇	RIIYIIRFL	MS
	F13L ₁₄₀₋₁₄₉	SIHTIKTLGV	MS
	J6R ₃₇₅₋₃₈₄	SIIFGGRQPSL	MS
	K1L ₁₉₁₋₂₀₀	SLLFIPDIKL	MS
	D10R ₁₆₈₋₁₇₆	TIINKFFEV	MS
	G4L ₅₇₋₆₆	TLIGNFAAHL	MS
	A50R ₄₅₈₋₄₆₆	TLRVLQDQL	MS
	F1L ₁₂₅₋₁₃₃	TVYDINNEV	MS
	D13L ₇₀₋₇₈	VLSLELPLEV	MS
	I1L ₁₂₂₋₁₃₀	YIDISDVKV	MS
	D1R ₇₆₄₋₇₇₂	YIIKKNDIV	MS
	D13L ₆₂₋₇₀	YITALNHLV	MS
	E6R ₄₆₂₋₄₇₀	YLDGQLARL	MS
	A31R ₆₈₋₇₆	TINDLKMM	MS
	A8R ₁₃₄₋₁₄₂	QVSIIQEKL	MS
	N/A	TVMINNVKI	dMS
	A7L ₂₄₉₋₂₅₇	TVMINNVKL	MS
	K3L ₅₇₋₆₅	KLVGKTVKV	MS
	O1L ₅₅₀₋₅₅₉	PITDSLSFKL	MS
	D12L ₁₇₄₋₁₈₂	SLFKNRVLL	MS+
	A orf A ₁₀₂₋₁₁₀	YLFLICHNL	MS
	D5R ₅₆₈₋₅₇₇	KIRSDNIKKL	MS

B. B*07;02

	ORF	Peptide	Source
Pool 1	D11L ₁₀₂₋₁₁₁	APEITKDCIF	MS
	B17L ₁₈₂₋₁₉₁	APLPGNVLVY	MS
	N/A	APYPGNVLVY	dMS
	F4L ₆₋₁₄	APNPNRFVI	Public
	B8R ₁₅₈₋₁₆₇	EPVTYDIDDY	MS
	N/A	EPVTYNIDDY	dMS
	N/A	B35	MS
	B8R ₇₀₋₇₈	FPKNDVFVSF	MS
	N/A	B35	MS
	E9L ₁₇₅₋₁₈₃	FPSVFINPI	MS
	N/A	FPSVFINPV	dMS
	E9L ₅₂₆₋₅₃₄	FPYEGGKVF	MS
	N/A	B35	MS
	I1L ₁₈₄₋₁₉₂	IPDELIDVL	MS
	J6R ₁₁₀₃₋₁₁₁₁	IPISDYTGY	MS
	N/A	B35	MS
	F2L ₄₂₋₅₀	IPPGERQLI	MS
	D9R ₂₆₋₃₅	IPRSKDTHVF	MS
	C19L/B25R ₇₈₋₈₆	NPSVLKILL	MS
	G9R ₁₄₋₂₃	PPPGVPTDEM	MS
	F2L ₂₆₋₃₅	SPGAAGYDLY	MS
	G9R ₆₉₋₇₇	GPGLSALL	MS
	B15R ₉₁₋₁₀₁	IPDEQKTIIGL	Predicted
	A20R ₁₆₂₋₁₇₀	IPKYLEIEI	MS
	N/A	B35	MS
	N/A	B35	MS

Pool 2	J5L ₅₃₋₆₁	LPASLKKNI	MS
	H1L ₆₅₋₇₃	LPNSNINII	MS
	A10L ₁₂₂₋₁₃₀	LPPFTQHLL	MS
	J6R ₃₀₃₋₃₁₁	MPAYIRNTL	Public
	A40R ₈₈₋₉₆	NPNSDLIKI	MS
	E5R ₁₃₁₋₁₄₀	NPSKMVYALL	MS
	N/A	NPSKMAYALL	dMS
	N/A	B35	MS
	N/A	NPVTINEY	dMS
	B18R ₃₀₅₋₃₁₃	RPADSITYL	MS
	N/A	RPLDSITYL	dMS
	D1R ₈₀₈₋₈₁₇	RPSTRNFFEL	MS+
	I8R ₂₂₁₋₂₃₀	RPVILSLPRI	MS
	N/A	B35	MS

ORF^a	Peptide	Source^b
A3L ₁₉₂₋₂₀₀	SPSNHHILL	MS
H5R ₈₉₋₉₇	SPSPGVGDI	MS
N/A	B35	MS
G7L ₁₇₅₋₁₈₃	LPMIIGEPI	MS
N/A	B35	MS
I7L ₃₄₂₋₃₅₀	TPPKSFKSL	MS
B22R ₇₂₋₈₀	TVADVRHCL	Public
J3R ₂₅₃₋₂₆₁	YPNQEYDYF	MS
A4L ₁₂₆₋₁₃₅	APASSLLPAL	MS
B12R ₂₅₁₋₂₅₉	EPELVRVYI	MS
A16L ₃₃₀₋₃₃₉	EPVVVKDKIKL	MS
O1L ₅₄₉₋₅₅₇	IPITESLSF	Public

Pool 3	N/A	IPNYLEIEI	dMS
	N/A	B35	MS
	C1L ₁₀₂₋₁₁₁	KPKPAVRFAI	Public
	A24R ₁₀₀₂₋₁₀₁₀	KPYASKVFF	MS
	C10L ₄₁₋₄₉	LPMEDNSDI	MS
	E1L ₁₀₋₁₈	LPNITLKII	MS
	D11L ₅₀₆₋₅₁₄	MPTVDEDLF	MS
	C20L/B26R ₇₋₁₆	EPIRGYVIIL	MS
	G5R ₃₄₁₋₃₄₉	LPCQLMYAL	MS
	D5R ₃₆₁₋₃₆₉	EPLITKLIL	MS
	N/A	B35	MS
	D1R ₆₈₆₋₆₉₄	HPRHYATVM	Public
	J6R ₁₀₈₉₋₁₀₉₈	LPGAANKGKI	MS
	A10L ₁₁₁₋₁₂₀	NPIINTHSFY	MS
	O1L ₃₃₅₋₃₄₄	RPMSLRSTII	Public
	A3L ₄₅₃₋₄₆₂	SPVIVNGAMM	MS
	I6L ₂₃₇₋₂₄₅	FPTNTLTSI	MS
	D1R ₃₈₄₋₃₉₃	GPKSNIDFKI	MS
	K6L ₁₇₋₂₅	KPITYPKAL	MS
	I4L ₄₉₈₋₅₀₇	RPIGIGVQGL	MS
	N2L ₁₀₄₋₁₁₃	RPNQHHTIDL	MS
	A34R ₈₂₋₉₀	LPRPDTRHL	MS+
	E2L ₂₁₆₋₂₂₄	RPRDAIRFL	MS
	H3L ₆₋₁₄	TPVIVVPVI	MS
	G2R ₁₄₀₋₁₄₉	VPITGSKLIL	MS
	A11R ₂₂₋₃₀	YPSNKNYEI	MS

Pool 4	N/A	APAAPGLSL	self
	N/A	APIDRVGQTL	self

ORF^a	Peptide	Source^b
N/A	APKCDVSFL	self
N/A	EPTPGPVRIL	self
N/A	GPSGLGKTAI	self
N/A	GPVRPYFSL	self
N/A	IPRDPSQQEL	self
K1L ₁₅₁₋₁₅₉	IPSTFDLAI	MS
N/A	KPRPDVTNEL	self
N/A	LPAESLGPRI	self
B16R ₂₂₆₋₂₃₄	LPDGIVTSI	MS
N/A	LPNELPAHLL	self
N/A	LPQANRDTL	self
N/A	LPRKPVAGAL	self
N/A	RPFPKLRIL	self
N/A	LPVSCTPGPL	self
N/A	RPGSSDRVL	self
N/A	RPQASHQLL	self
N/A	RPQVAKTLL	self
N/A	RPRPVSPSSL	self
N/A	RPSPPNPEL	self
N/A	SPAGSTRVL	self
N/A	SPNDKSINAL	self
N/A	SPRAAEPVQL	self
N/A	SPSSKYVKL	self
N/A	APRKGSFSAL	self

Pool 5	A4L ₈₃₋₉₁	VPTATPAPI	MS
	E6R ₂₈₄₋₂₉₃	EPEKDIRELL	MS
	N/A	B35	MS
	D1R ₃₈₄₋₃₉₃	GPKSNIDFKI	MS
	I6L ₂₇₂₋₂₈₀	IPKKIVSLL	MS
	A40R ₃₋₁₁	KPKTDYAGY	MS
	A47L ₂₂₇₋₂₃₆	KPVSDLYTSM	MS
	N/A	B35	MS
	D5R ₃₇₅₋₃₈₃	LPKEYSSEL	MS
	N/A	B35	MS
	D8L ₁₆₀₋₁₆₉	LPSKLDYFTY	MS
	N/A	APIQGNREEL	self
	N/A	APSAFGMML	self
	N/A	LPKTGTVSL	self
	N/A	SPSSPGSSL	self
	N/A	SPVYLLAYL	self
	N/A	TPSNTPTGPL	self
	L4R ₃₇₋₄₅	FPRSMLSIF	MS

ORF ^a	Peptide	Source ^b
J3R ₈₋₁₆	KPFMYFEEI	MS
N/A	KPYFPPRIL	self
N/A	LPSKPSSTL	self
D9R ₁₀₀₋₁₀₉	DPHFEELILL	MS
G5R ₃₄₁₋₃₄₉	LPCQLMYAL	MS
C10L ₄₁₋₅₀	LPMEDNSDII	MS
I6L ₂₈₂₋₂₉₁	LPSNVEIKAI	MS
N/A	B35	MS
N/A	B35	MS
N/A	B35	MS
A11R ₂₂₋₃₀	YPSNKNYEI	MS

^aORFs are defined as in Table 1, asterisks indicated peptides homologous to Western Reserve (VACWR, ID 696871) or Ankara (VACCA, ID 126794) vaccinia strains;

^bPrior reports according to the immune epitope data base (IEDB; www.iedb.org). MS, this study; dMS, derivatives of MS-discovered VACV peptides generated as homologous to variola virus (Reference ID 10255). MS+, reported from MHC class I ligand elution; public, reported as positive in human or HLA class I transgenic mouse TCD8 assay; predicted, reported as predicted VACV epitopes; B35, naturally processed HLA-B35 restricted VACV peptides found in this study (unpublished data); self, self peptides found to be naturally presented by VACV-infected HeLa cells in this study

Supplementary Table 4. Summary of immune epitopes identified in smallpox-vaccinated volunteers

A*02;01

Sequence	V001	V008	V023	V034	V115	V163	V168
<i>Novel immune epitopes identified in this study</i>							
AINVEKIEL							224
DIDEILEKV		113					
MIKPCCERV	155						
KIEDLINQL		153					
LILDPKINV		100					
RIIYIIRFL	124				112		
TLIGNFAAHL	653	207					
VLISPVSIL		231	189				
YIDISDVKV	282						
KLTFLDVEV	111						
ILNDEQLNL	408	1222					
SLYNLVKSSV					263		
YITALNHLV					225		
KISNTTFEV	115						
YLDGQLARL					225		
KIDDMIEEV		116					
KLVGKTVKV					112		
SLSNLDFRL	*226	*100	*119				115
SLLFIPDIKL	520						
LIQEIVHEV	226						
<i>Known immune epitopes also found as naturally processed in this study</i>							
VLEDVQAAGI		133					
FLTSVINRV	*877	*136	*249	*245			
ILDDNLYKV	*1162	*2602	*5362	*2839			
SLFKNVRL					112		
RVYEALYYV	*297						
WLIGFDFDV	188						
IVIEAIHTV			*288	*625			
KVDDTFYYV	*453		*928	*156			
NLFDIPLLT	*388	*256	*171	*903			
KIDYYIPYV	*1836	*344	*925	*379			
GLNDYLHSV	*308	*518	*1069	*778			

Supplementary Table 4 contd...

Known immune epitopes not found as naturally processed in this study

VLPDFDIKKL	107			
TLFPGDDDL				182
TLLDHIRTA	*320		*1036	
YIYGIPSL			2909	
CLTEYILWV	*1360	*2229	*1892	*2009
YLPEVISTI		176		
ALDEKLFLI			*445	*195
GLDFVNPFV			*195	

The HLA class I allotype for each donor is provided in Table S2

The numbers of spot forming cells (SFC) over background per million PBMCs that secrete IFN- γ in response to individual peptides are presented

Responses are considered positive if SFC cells per million PBMC were at least 100 over background

*Epitopes also found as positive in tetramer binding assay

Supplementary Table 5. Summary of immune epitopes identified in HLA class I transgenic mice

A*02;01

Sequence ^a	ORF	t _{1/2} , h
<i>Novel immune epitopes identified in this study</i>		
YIDISDVKV	I1L ₁₂₂₋₁₃₀	0.82
SLSNLDFRL*	F11L ₃₄₀₋₃₄₈	23.58
TLIGNFAAHL	G4L ₅₇₋₆₆	9.86
TLRVLQDQL	A50R ₄₅₈₋₄₆₆	0.19
KIDDMIEEV*	C9L ₆₀₂₋₆₁₀	9.34
VLSLELPNV*	D13L ₇₀₋₇₈	22.73
DLKPDNILL*	F10L ₃₀₇₋₃₁₅	ND
<i>Known immune epitopes also found as naturally processed in this study</i>		
ILSDENYLL*	A6L ₁₇₁₋₁₇₉	24.41
KLFSDISAI*	E5R ₁₁₇₋₁₂₅	17.75
RLYDYFTRV*	I1L ₂₁₁₋₂₁₉	20.04
VLYDEFVTI*	A6L ₆₋₁₄	14.04
ILDDNLYKV*	G5R ₁₈₋₂₆	26.21
HVDGKILFV*	B13R ₃₂₇₋₃₃₅	4.22
SLSAYIIRV*	H3L ₁₈₄₋₁₉₂	25.52
RVYEALYYV*	D12L ₂₅₁₋₂₅₉	14.44
NLFDIPLLTV*	F12L ₂₈₆₋₂₉₅	22.59
IVIEAIHTV*	A48R ₂₁₀₋₂₁₈	6.66
KVDDTFYYV*	C7L ₇₄₋₈₂	12.21
<i>Known immune epitopes not found as naturally processed in this study</i>		
ALDEKLFLI*	A23R ₂₇₃₋₂₈₁	ND
GLFDFVNPFV*	A46R ₁₄₂₋₁₅₀	24.76

^aIdentified by IFN- γ ELISpot assay

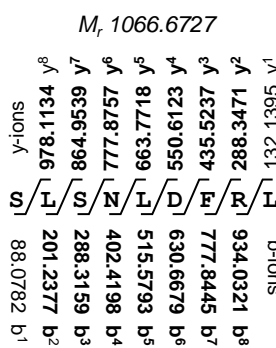
*Epitopes also found as positive in tetramer binding assay

Supplementary Figure 1. Identification of vaccinia viral determinants presented during active infection.

Representative mass spectra comparing synthetic peptides with the peptides eluted from purified sA2.1 (**A**) and sB7.2 molecules (**B**; Native). For each spectrum, the *b*- and *y*-ion fragments are indicated along with the Sequest cross-correlation score (Cn) showing the degree of concordance between the observed and expected fragment patterns. To the left of the spectra are the ion values for each peptide (**bold**, observed ion masses).

Supplementary Figure 1

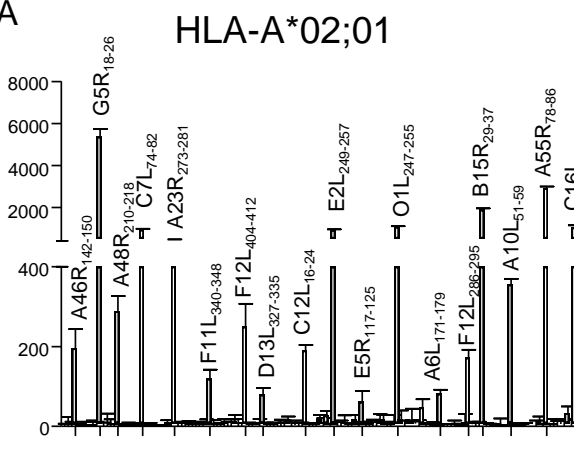
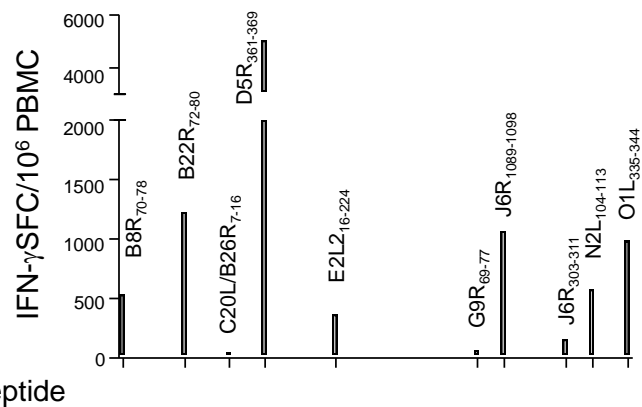
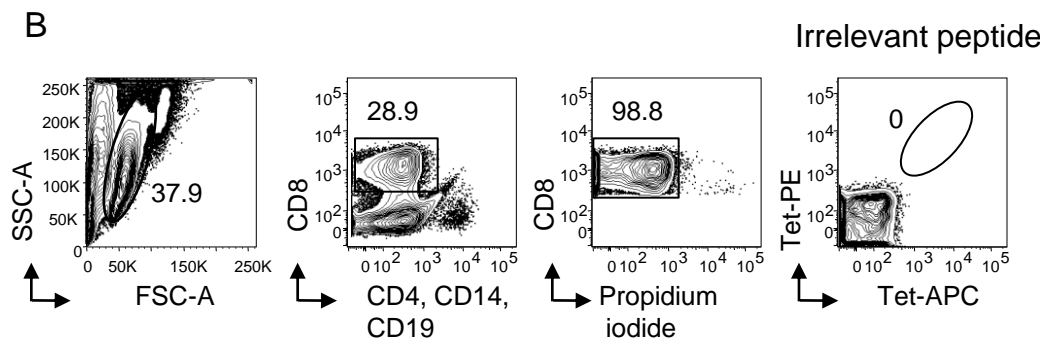
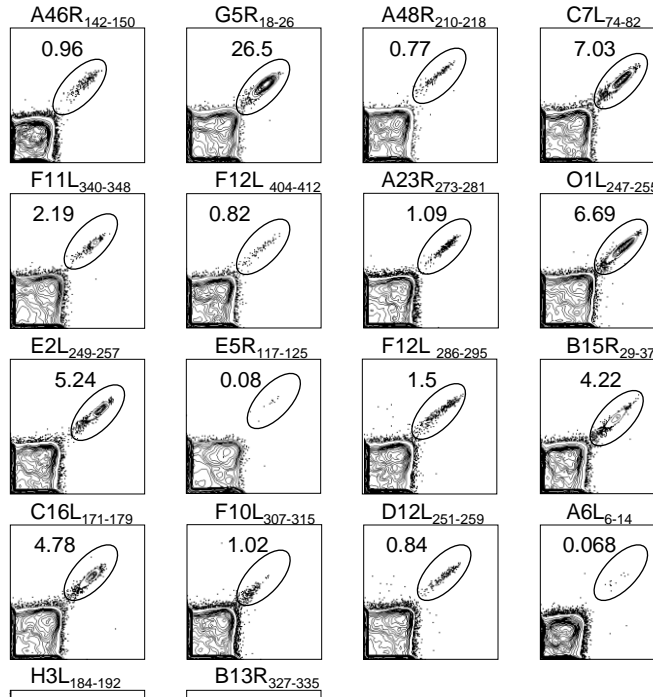
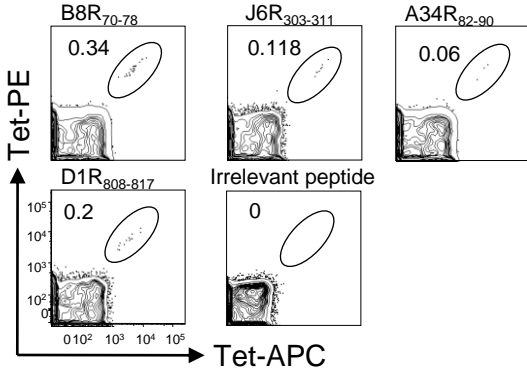
A



Supplementary Figure 2. Identification of vaccinia-specific TCD8 responses in smallpox-vaccinated volunteers.

PBMCs were expanded ex vivo with peptide pools (Table S4) and the immune epitopes were identified using IFN- γ ELISpot assay (**A**) and by dual-fluorochrome encoding using the indicated PE- and APC-conjugated p/B7.2 tetramers (**B–C**). Bar graph indicates mean \pm SD of the assay duplicates. Contour plots were gated on live CD8 $^{+}$ T lymphocytes as shown in (**B**). Irrelevant peptide is a B*07;02-restricted HMPV immune epitope (13).

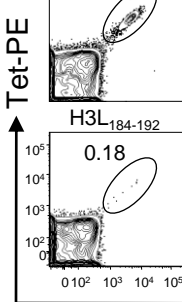
Supplementary Figure 2

A**HLA-B*07:02****B****C****HLA-A*02:01****HLA-B*07:02**

Tet-PE

↑

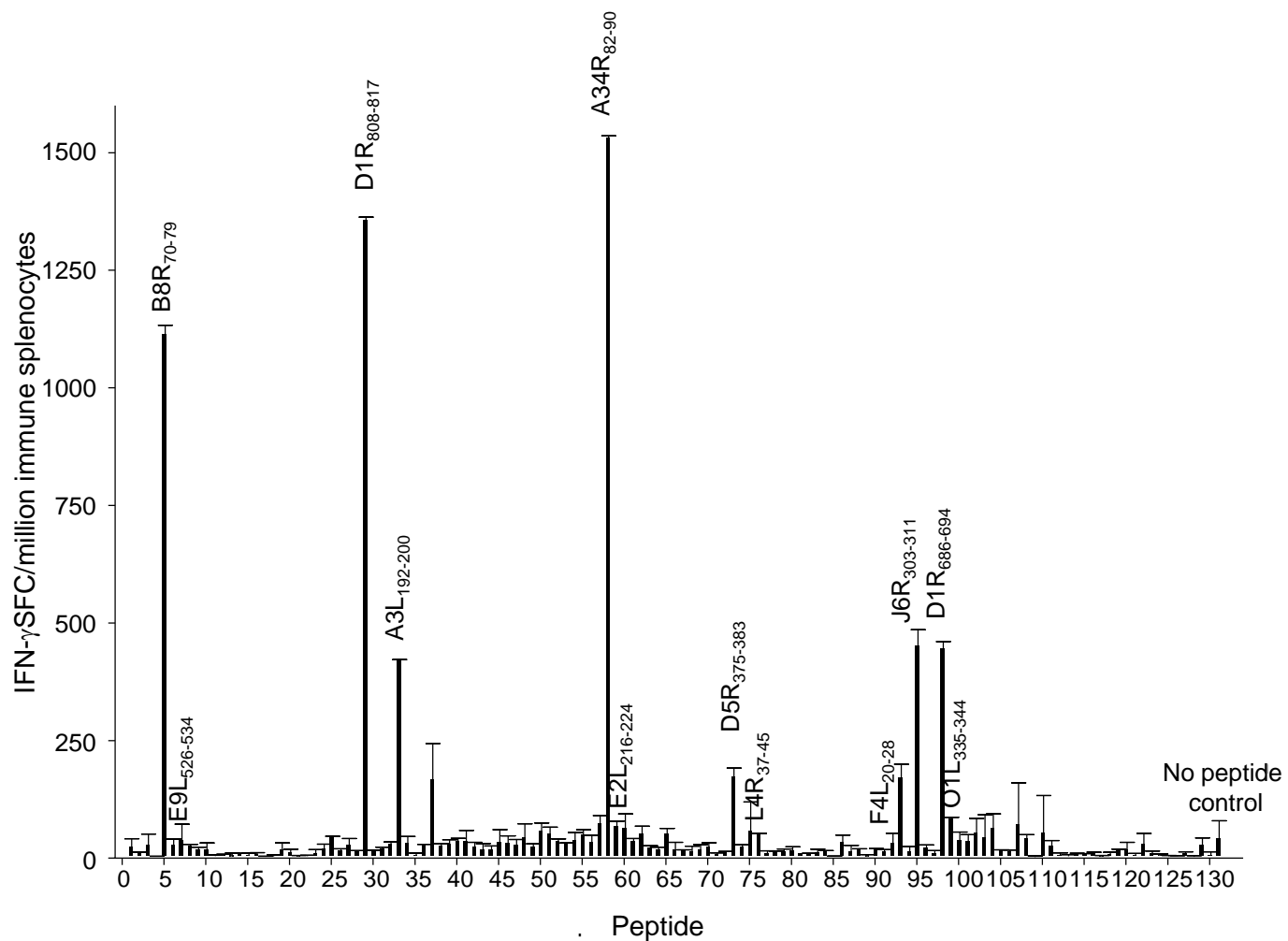
Tet-APC



Supplementary Figure 3. Identification immune TCD8 elicited by VACV in HLA class I transgenic mice.

A2^{tg} mice were inoculated i.p. with VACV and splenic TCD8 responses were analyzed on d7 p.i. using IFN- γ ELISpot assay. Data are representative of at least three independent experiments; $n=3-5$ mice/experiment; mean \pm SD.

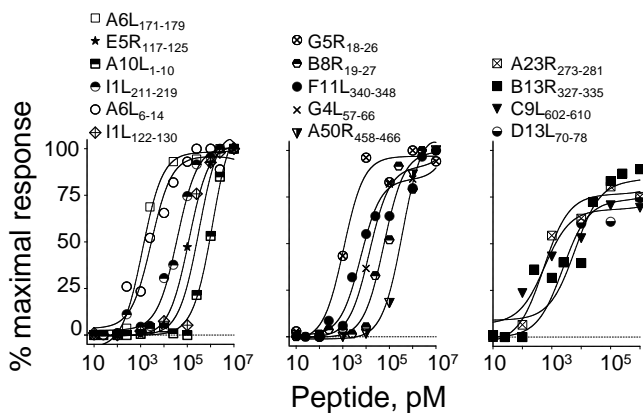
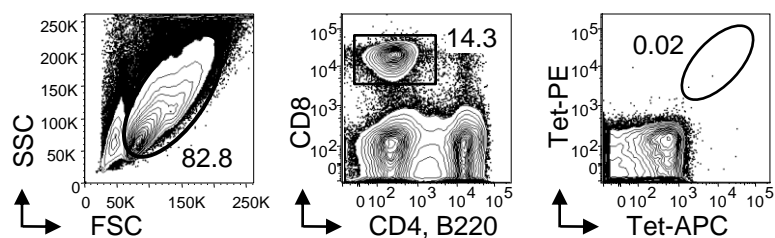
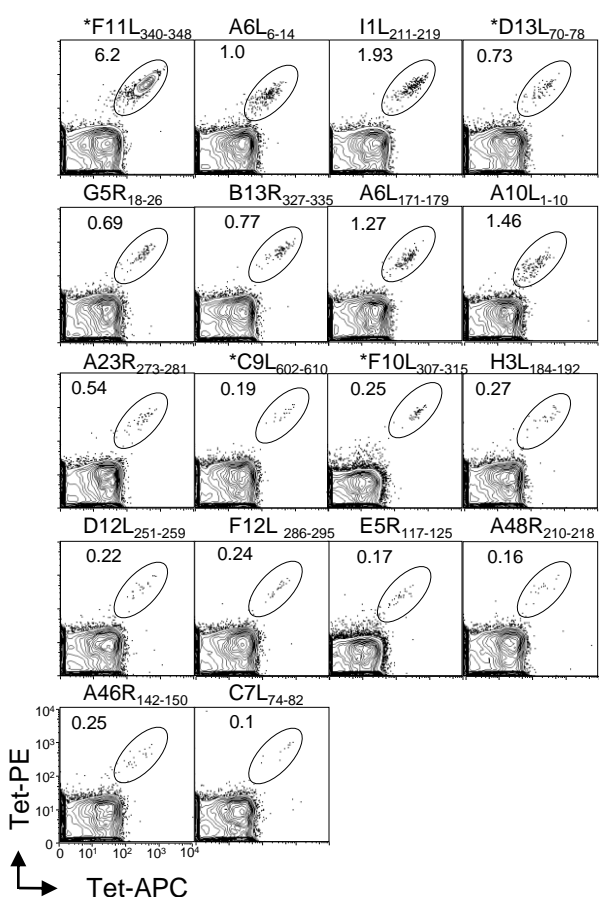
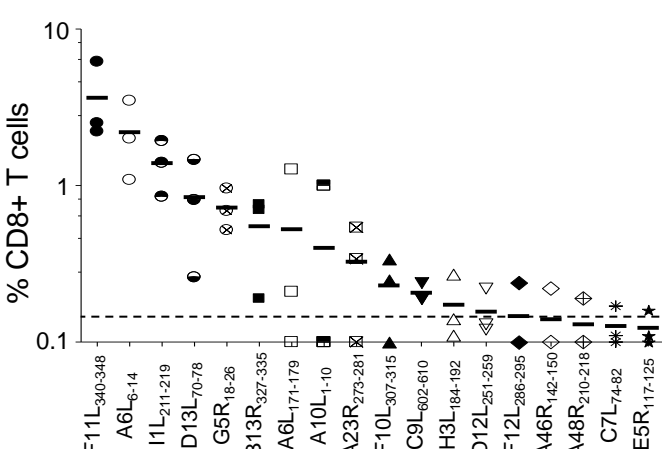
Supplementary Figure 3



Supplementary Figure 4. Validating VACV-specific TCD8 responses in HLA A02;01 transgenic mice.

A2^{tg} mice were inoculated i.p. with VACV and splenic TCD8 responses were analyzed on d7 p.i.

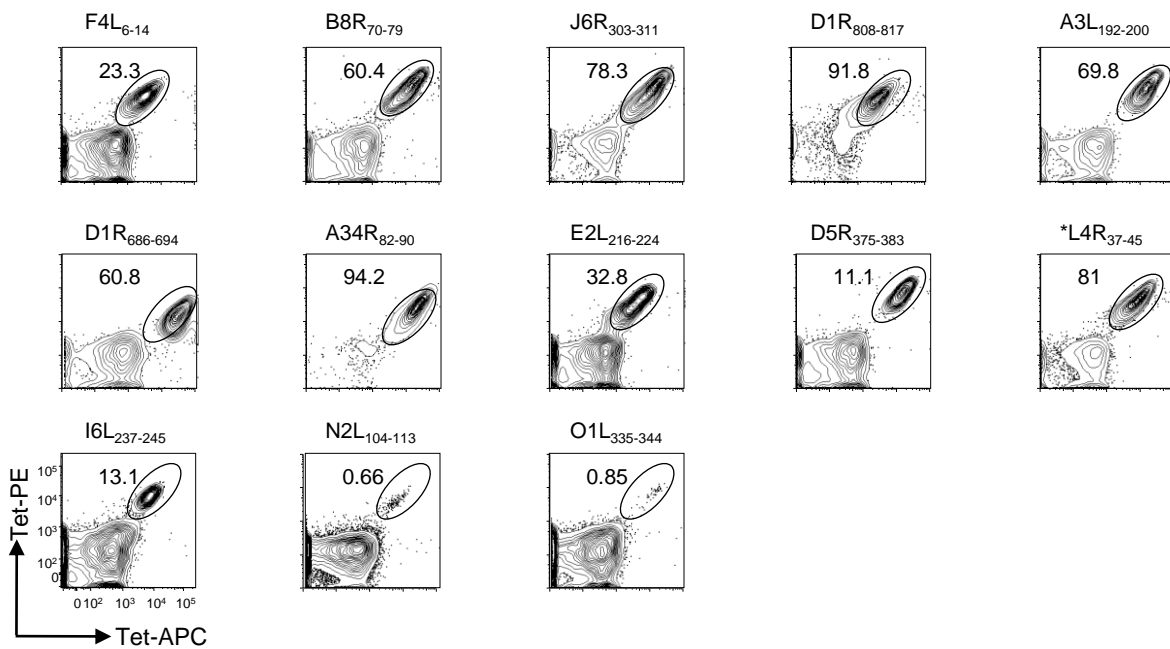
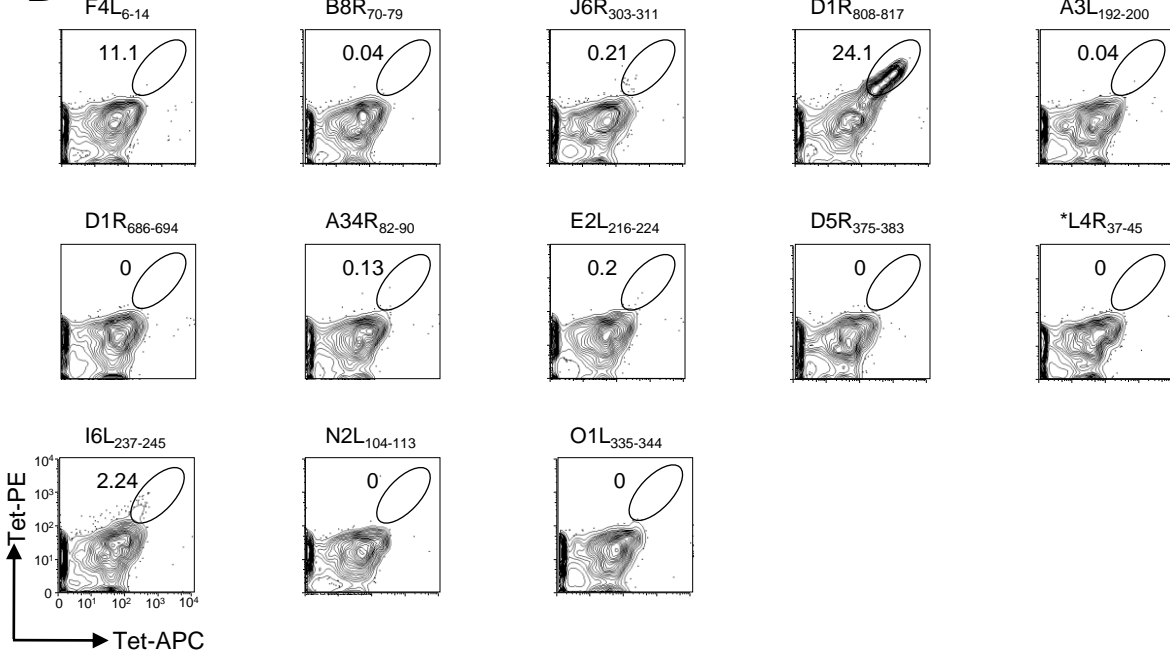
- (A) Dose-dependent IFN- γ response by VACV-immune splenocytes measured by epitope titration in the ELISpot assay. Data represent the mean of triplicate wells; representative of two independent experiments ($n=5$).
- (B) Gating strategy utilized for identification of individual TCD8 specificities with tetramers from mouse immune splenocytes.
- (C) TCD8 responses detected using p/class I tetramers on VACV immune splenocytes. Representative of 3 independent experiments using pooled spleens ($n=5-10$). Numbers indicate % CD8⁺ p/class I tetramer+ cells; *, novel immune epitopes.
- (D) VACV-specific TCD8 hierarchy defined by p/class I tetramer staining of VACV immune splenocytes. Cumulative data from 3 experiments ($n=5-8$). Each dot represents TCD8 frequency from one experiment. Dotted line indicates assay background defined by irrelevant HMPV-derived TCD8 epitope/B7.2 tetramer binding (13).

A**B****Irrelevant peptide****C****D**

Supplementary Figure 5. Validating immune TCD8 identified in acutely infected B7^{tg} mice by their ability to expand in splenic cultures after re-stimulation with individual antigenic peptides.

Splenic cells of VACV immune or uninfected mice were expanded in vitro with individual antigenic peptides (100nM) in the presence of rhIL-2 (5U/ml). On d7, expansion of epitope specific TCD8 from VACV immune (A) and naïve (B) splenic cultures was monitored by flow cytometry using p/B7.2 tetramers. Contour plots are gated on live CD8⁺ T lymphocytes. Numbers indicate percent epitope-specific TCD8. Data are representative of two independent experiments; n=3 pooled spleens/experiment.

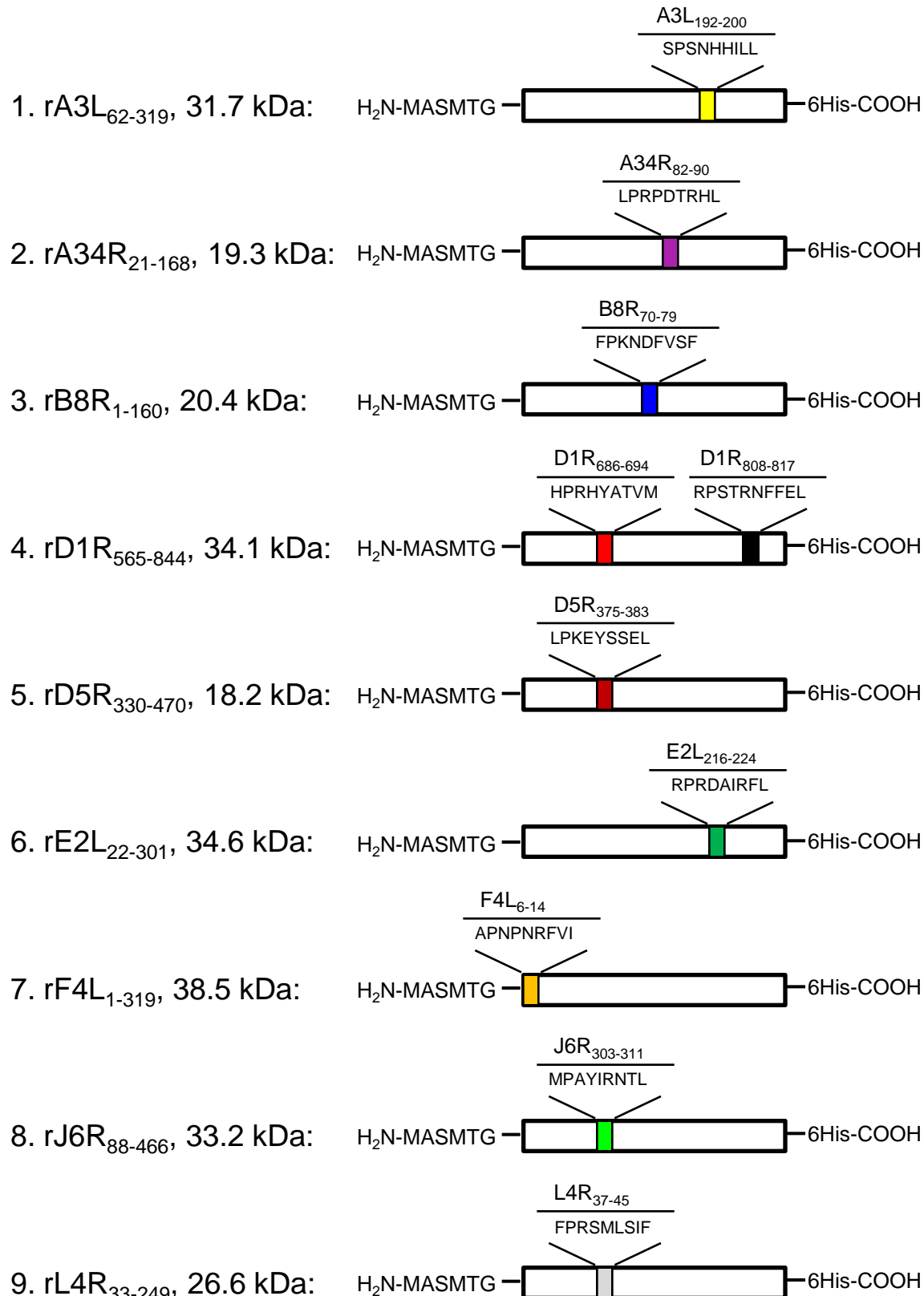
Supplementary Figure 5

A**B**

Supplementary Figure 6. Design of recombinant VACV-derived proteins encompassing targeted immune determinants.

Schematic diagram of engineered proteins showing nine VACV antigens with amino acid positions selected for the design of truncated recombinant subunit. Location and sequences of immune epitopes, and also their N- and C-terminal tag sequences introduced to facilitate expression and purification of recombinant proteins from *E. coli* are shown. Note that recombinant B8R₁₋₁₆₀ and A34R₂₁₋₁₆₈ were produced in undetectable amounts by *E. coli*.

Supplementary Figure 6



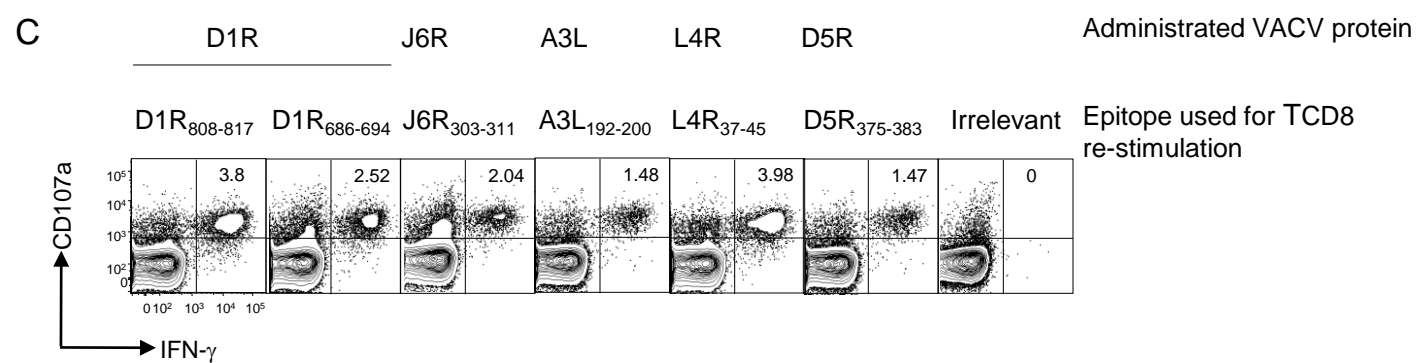
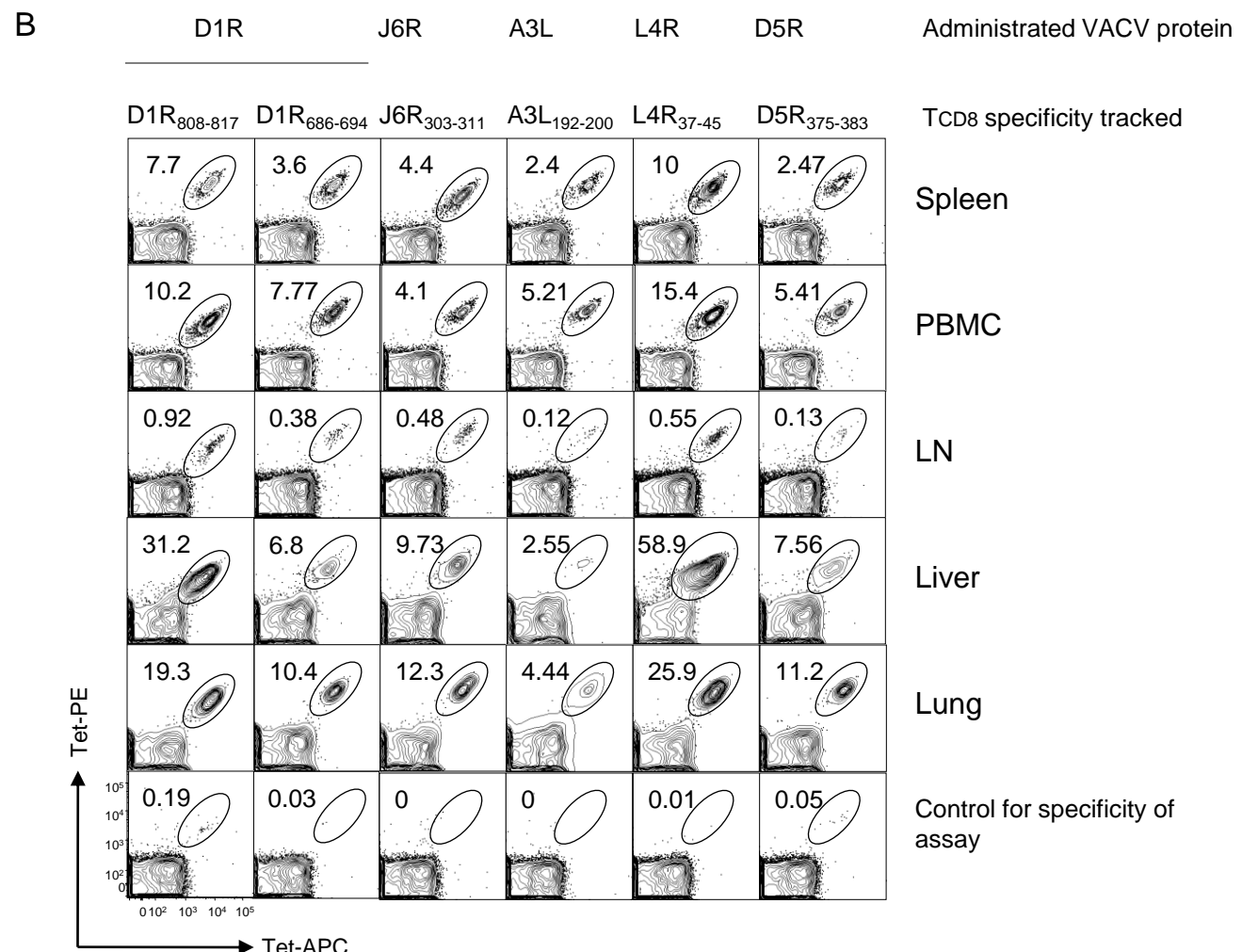
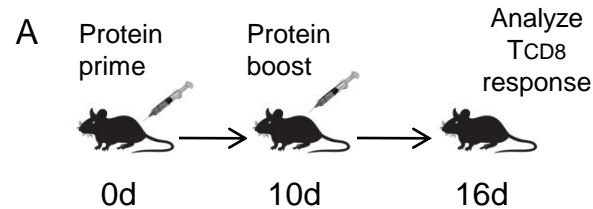
Supplementary Figure 7. Efficient processing of immune determinants from cognate VACV proteins

(A) Immunization strategy: Recombinant VACV-derived proteins containing targeted antigenic determinants were formulated with α GalCer and administrated to mice i.p. as indicated.

B) Robust systemic epitope-specific TCD8 response detected was with p/class I tetramers after prime-boost with individual VACV proteins. Data are representative of at least two independent experiments using pooled samples ($n=3-7$).

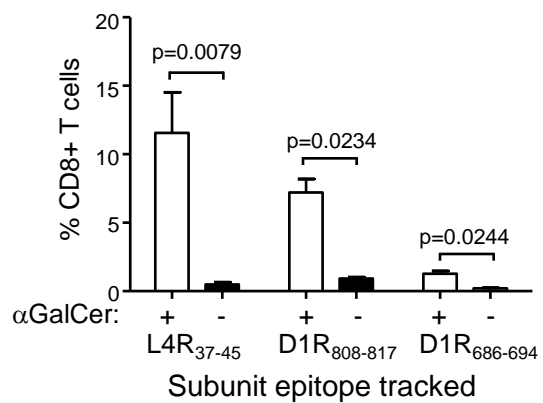
(C) TCD8 elicited after protein immunization functionally responded to re-stimulation with appropriate synthetic peptides by degranulation and production of intracellular IFN- γ .

Supplementary Figure 7



Supplementary Figure 8. Priming of TCD8 response with antigenic protein requires αGalCer in the protein-adjuvant formulation. Mice ($n=5/\text{group}$) were primed once i.p. with 20 μg of individual recombinant subunits (L4R₃₃₋₂₄₉ or D1R₅₆₅₋₈₄₄) with or without αGalCer (1 $\mu\text{g}/\text{mouse}$) and epitope-specific TCD8 against targeted epitopes were enumerated on d10 p.i. from blood with p/B7.2 tetramers. Each dot represents individual mouse. **, $p<0.01$ (Mann-Whitney); nd, not detected. Representative of two independent experiments.

Supplementary Figure 8

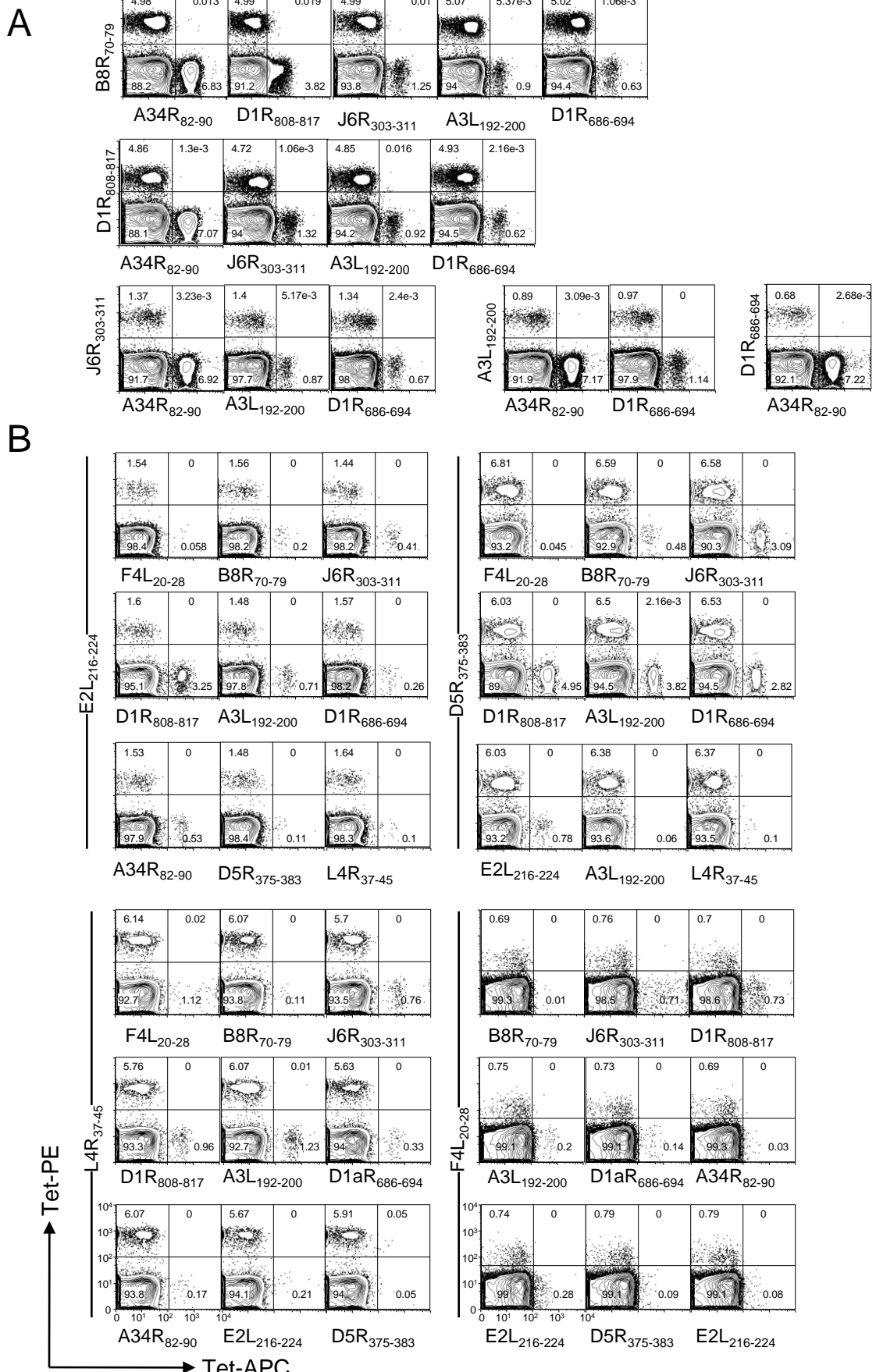


Supplementary Figure 9. Validating individual TCD8 specificities elicited by VACV using combinatorial exclusion flow cytometry with dual-fluorochrome-encoded p/B7.2 tetramers.

(A) Primary TCD8 response analyzed on d7 p.i.

(B) Four subdominant TCD8 were enhanced by priming with peptides followed by VACV challenge before analysis. Contour plots are gated on live CD8⁺ T lymphocytes. Gate numbers indicate percent epitope-specific TCD8. Data are representative of two independent experiments; $n=5$ mice/experiment.

Supplementary Figure 9



Supplementary Figure 10. Characterization of TCD8 response elicited in acutely infected B7^{tg} mice.

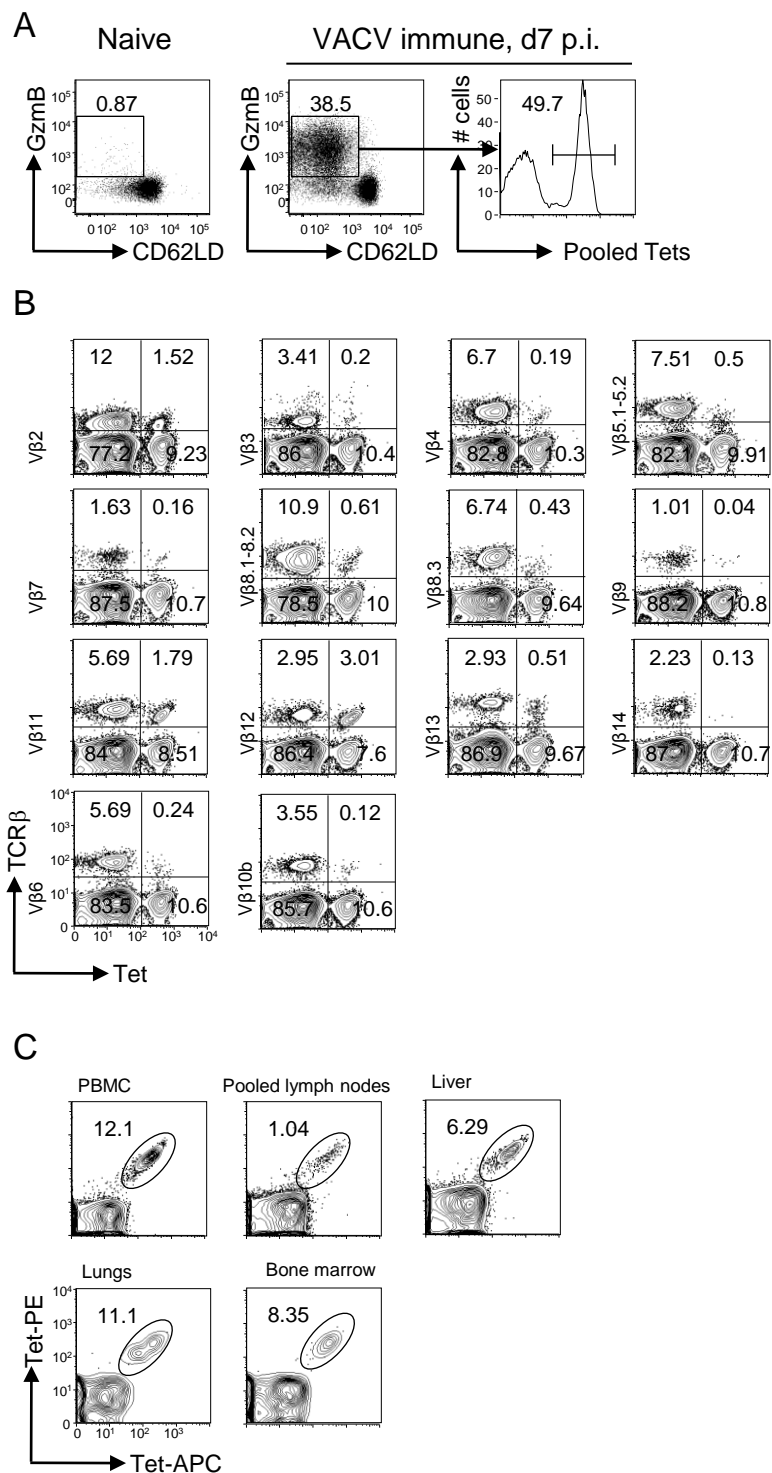
Mice were inoculated i.p. with 2×10^5 pfu VACV and TCD8 response was analyzed as indicated below.

(A) Coverage of the overall anti-VACV response by identified TCD8 specificities determined as the fraction of the CD44^{HI}CD62L^{LO}GzmB⁺ population within splenic TCD8 population stained by pooled p/B7.2 tetramers against 10 immune determinants as in Figure 3. Measurement was performed on individual mouse ($n=5$). Data are representative of two independent experiments.

(B) Analysis of TCR V β usage within a given TCD8 specificity revealed multiple clonotypes. Cells were gated on live CD8⁺ T lymphocytes.

(C) Anti-VACV epitope-specific TCD8 detected in lymphoid and peripheral tissues. Data are representative of at least three independent experiments; $n=3-5$ mice/experiment for A34R₈₂₋₉₀-specific TCD8 in B and C.

Supplementary Figure 10

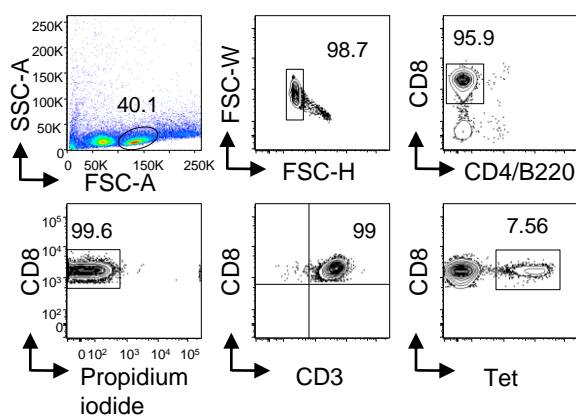


Supplementary Figure 11. Enumeration of naïve pTCD8 specific to VACV determinants in B7^{tg} mice.

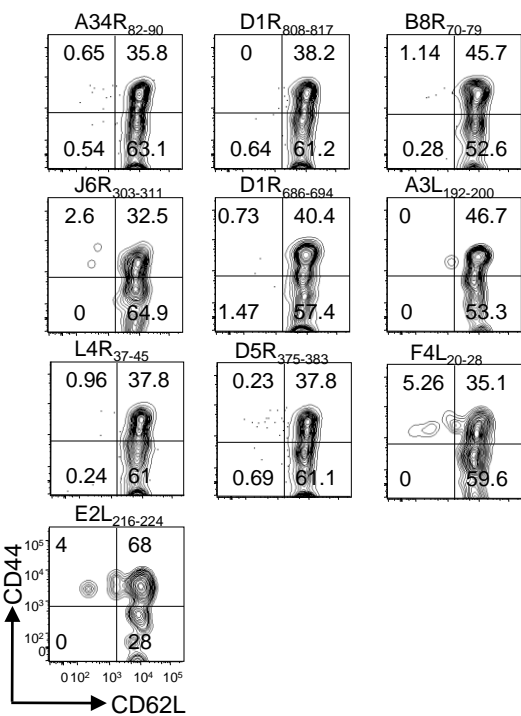
- (A) Flow cytometry gating strategy used to identify naïve TCD8 from total pooled spleen and lymph node cells: FSC/SSC-A, FSC-(W/H)^{LO} SSC-(W/H)^{LO}, B220^{NEG}/CD4^{NEG}/CD8α⁺/CD3ε⁺, PI^{LO} and p/B7.2 tetramer⁺. Representative flow plots to identify L4R₃₇₋₄₅-specific pTCD8 are shown.
- (B) Representative flow plots for ten pTCD8 specificities enriched with p/B7.2 tetramers are shown.
- (C) Phenotype of epitope-specific naïve pTCD8 enriched with p/B7.2 tetramers. Contour plots are gated on p/B7.2 class I tetramer⁺ cells.
- (D) Normalized frequency of naïve pTCD8 for the naturally processed VACV determinants identified in B7^{tg} mice (HLA-B7^{tg} mouse has ~8.3x10⁶ total naïve CD8⁺ T cells compared to C57BL/6 mice, which have ~17x10⁶ total naïve CD8⁺ T cells). Data represent 3–5 independent experiments from pooled spleen and macroscopical LNs. Each dot represents one experiment; number indicates mean pTCD8 frequency per million CD8⁺ T cells.

Supplementary Figure 11

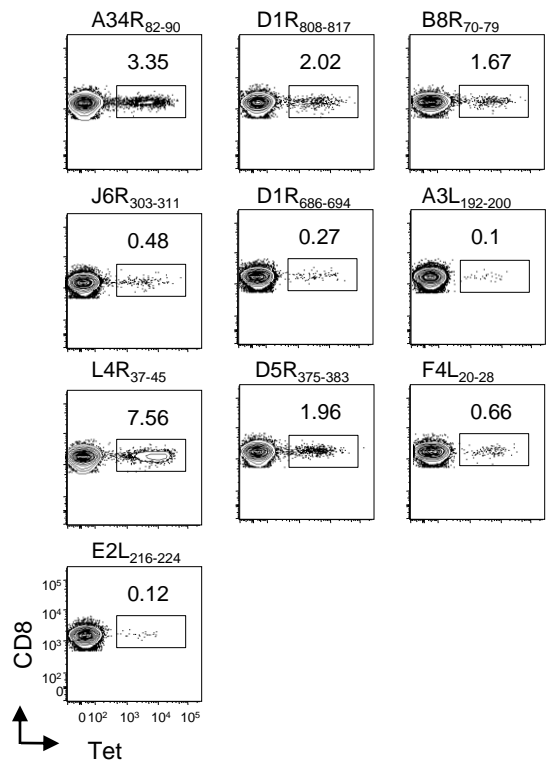
A



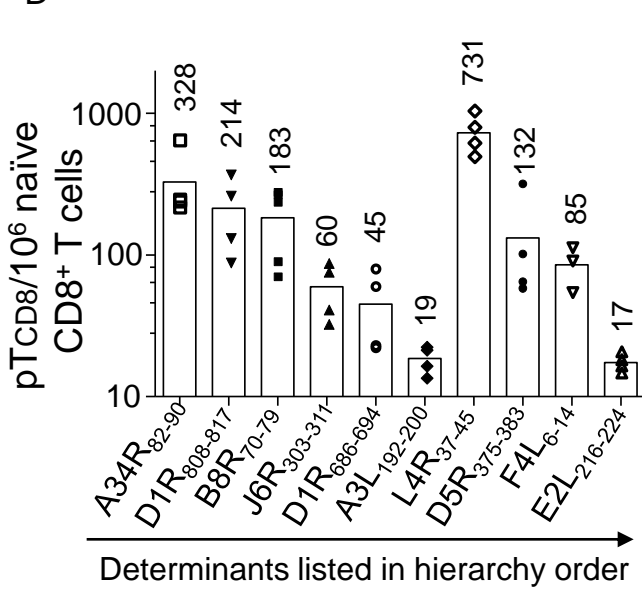
C



B



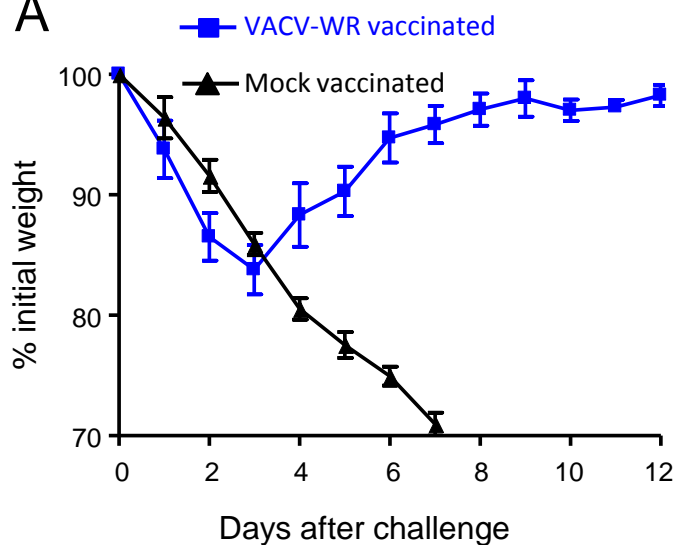
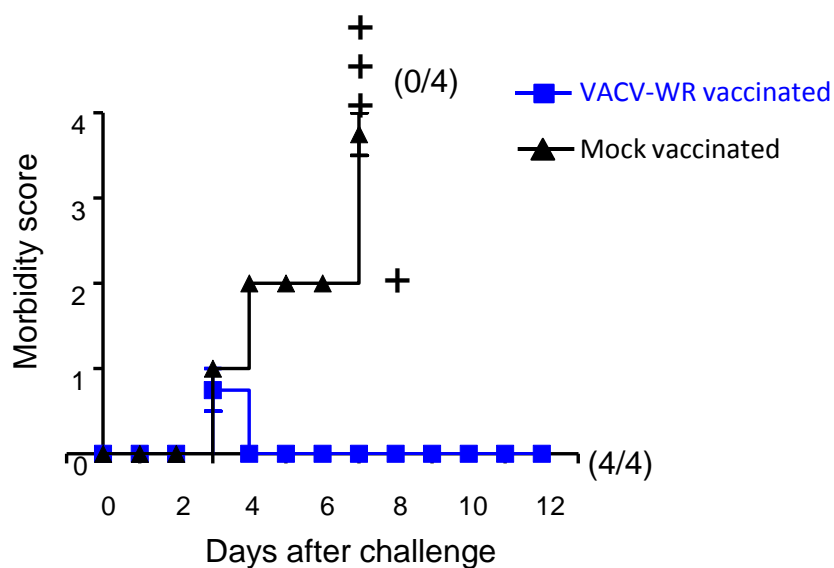
D



Supplementary Figure 12. Validation of VACV-WR inoculation conditions used for lethal respiratory challenge of epitope-vaccinated B7^{tg} mice shown in Figure 5A.

Two groups of B7^{tg} mice ($n=4-7/\text{group}$) were vaccinated with 10^6 pfu VACV-WR in 100 μl PBS (i.p.) or 100 μl PBS (i.p.). On d14 p.i., mice were anesthetized with ketamine/xylazine, challenged i.n. with 10^6 pfu VACV-WR in 50 μl PBS and observed during next 12 days for weight loss (A) and morbidity (B); mean \pm SEM. +, the time points at which death occurred between watch; the number of surviving/total animals are in parenthesis.

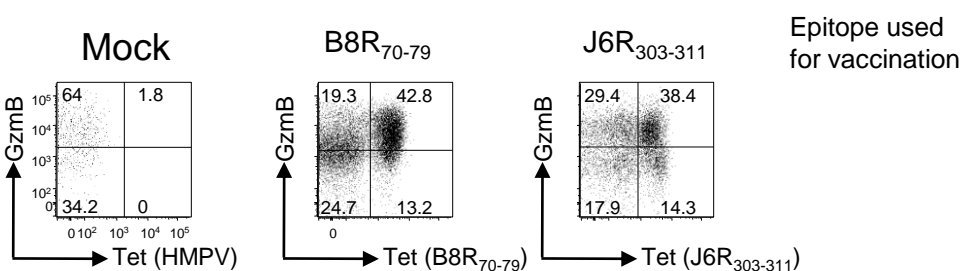
Supplementary Figure 12

A**B**

Supplementary Figure 13. Epitope-specific TCD8 elicited in lungs by peptide vaccination contain GzmB.

p/B7.2 tetramer staining of TCD8 harvested from infected lungs of non-vaccinated (mock) and epitope-vaccinated (B8R₇₀₋₇₉ and J6R₃₀₃₋₃₁₁) mice as in Figures 5, 6. The majority of TCD8 infiltrating lungs are specific for the single epitope targeted by vaccination and produce GzmB. Data represent one of five mice from each group.

Supplementary Figure 13



Literature Cited

1. Rodenko, B., Toebe, M., Hadrup, S.R., van Esch, W.J., Molenaar, A.M., Schumacher, T.N., and Ova, H. 2006. Generation of peptide-MHC class I complexes through UV-mediated ligand exchange. *Nat Protoc* 1:1120-1132.
2. Bakker, A.H., Hoppes, R., Linnemann, C., Toebe, M., Rodenko, B., Berkers, C.R., Hadrup, S.R., van Esch, W.J., Heemskerk, M.H., Ova, H., et al. 2008. Conditional MHC class I ligands and peptide exchange technology for the human MHC gene products HLA-A1, -A3, -A11, and -B7. *Proc Natl Acad Sci U S A* 105:3825-3830.
3. Toebe, M., Rodenko, B., Ova, H., and Schumacher, T.N. 2009. Generation of peptide MHC class I monomers and multimers through ligand exchange. *Curr Protoc Immunol* Chapter 18:Unit 18 16.
4. Hickman, H.D., Batson, C.L., Prilliman, K.R., Crawford, D.L., Jackson, K.L., and Hildebrand, W.H. 2000. C-terminal epitope tagging facilitates comparative ligand mapping from MHC class I positive cells. *Hum Immunol* 61:1339-1346.
5. Prilliman, K., Lindsey, M., Zuo, Y., Jackson, K.W., Zhang, Y., and Hildebrand, W. 1997. Large-scale production of class I bound peptides: assigning a signature to HLA-B*1501. *Immunogenetics* 45:379-385.
6. Harndahl, M., Rasmussen, M., Roder, G., and Buus, S. 2010. Real-time, high-throughput measurements of peptide-MHC-I dissociation using a scintillation proximity assay. *J Immunol Methods*.
7. Hadrup, S.R., Toebe, M., Rodenko, B., Bakker, A.H., Egan, D.A., Ova, H., and Schumacher, T.N. 2009. High-throughput T-cell epitope discovery through MHC peptide exchange. *Methods Mol Biol* 524:383-405.
8. Hadrup, S.R., Bakker, A.H., Shu, C.J., Andersen, R.S., van Veluw, J., Hombrink, P., Castermans, E., Thor Straten, P., Blank, C., Haanen, J.B., et al. 2009. Parallel detection of antigen-specific T-cell responses by multidimensional encoding of MHC multimers. *Nat Methods* 6:520-526.
9. Moon, J.J., Chu, H.H., Hata, J., Pagan, A.J., Pepper, M., McLachlan, J.B., Zell, T., and Jenkins, M.K. 2009. Tracking epitope-specific T cells. *Nat Protoc* 4:565-581.
10. Matheu, M.P., Sen, D., Cahalan, M.D., and Parker, I. 2008. Generation of bone marrow derived murine dendritic cells for use in 2-photon imaging. *J Vis Exp*.

11. Assarsson, E., Sidney, J., Oseroff, C., Pasquetto, V., Bui, H.H., Frahm, N., Brander, C., Peters, B., Grey, H., and Sette, A. 2007. A quantitative analysis of the variables affecting the repertoire of T cell specificities recognized after vaccinia virus infection. *J Immunol* 178:7890-7901.
12. Assarsson, E., Greenbaum, J.A., Sundstrom, M., Schaffer, L., Hammond, J.A., Pasquetto, V., Oseroff, C., Hendrickson, R.C., Lefkowitz, E.J., Tscharke, D.C., et al. 2008. Kinetic analysis of a complete poxvirus transcriptome reveals an immediate-early class of genes. *Proc Natl Acad Sci U S A* 105:2140-2145.
13. Erickson, J.J., Gilchuk, P., Hastings, A.K., Tollefson, S.J., Johnson, M., Downing, M.B., Boyd, K.L., Johnson, J.E., Kim, A.S., Joyce, S., et al. 2012. Viral acute lower respiratory infections impair CD8+ T cells through PD-1. *J Clin Invest*.